Articles

Identification of the Protein Targets of the Reactive Metabolite of Teucrin A in Vivo in the Rat

Alexandra Druckova,[†,‡,§] Raymond L. Mernaugh,[†] Amy-Joan L. Ham,[†,||] and Lawrence J. Marnett*[,†,‡,§]

Departments of Biochemistry, Chemistry, and Pharmacology, A. B. Hancock Jr. Memorial Laboratory for Cancer Research, Vanderbilt Institute of Chemical Biology, Center in Molecular Toxicology, Vanderbilt-Ingram Cancer Center, and Mass Spectrometry Research Center, Vanderbilt University School of Medicine, Nashville, Tennessee 37232-0146

Received April 27, 2007

Covalent modification of proteins is associated with the toxicity of many electrophiles, and the identification of relevant in vivo protein targets is a desirable but challenging goal. Here, we describe a strategy for the enrichment of adducted proteins utilizing single-chain fragment variable (ScFv) antibodies selected using phage-display technology. Teucrin A is a furan-containing diterpenoid found in the herb germander that is primarily responsible for the herb's hepatotoxicity in rodents and humans following metabolic activation by cytochrome P450 enzymes. Conjugates of the 1,4-enedial derivative of teucrin A, its presumed toxic metabolite, with lysine- and cysteine-containing peptides were synthesized and used to select ScFvs from a rodent phage-displayed library, which recognized the terpenoid moiety of the teucrin-derived adducts. Immunoaffinity isolation of adducted proteins from rat liver homogenates following administration of a toxic dose of teucrin A afforded a family of proteins that were identified by liquid chromatography/tandem mass spectrometry. Of the 46 proteins identified in this study, most were of mitochondrial and endoplasmic reticulum origin. Several cytosolic proteins were found, as well as four peroxisomal and two secreted proteins. Using Ingenuity Pathway Analysis software, two significant networks involving the target genes were identified that had major functions in gene expression, small molecule biochemistry, and cellular function and maintenance. These included proteins involved in lipid, amino acid, and drug metabolism. This study illustrates the utility of chemically synthesized biological conjugates of reactive intermediates and the potential of the phage display technology for the generation of affinity reagents for the isolation of adducted proteins.

Introduction

Covalent adduction of proteins has been linked to the toxicity of many reactive metabolites that are generated upon the activation of xenobiotics by cytochrome P450 enzymes (*1, 2*). Likewise, protein damage by endogenous electrophiles, such as the lipid peroxidation product, 4-hydroxynonenal (4-HNE), is associated with a number of human diseases, including neurological and autoimmune disorders, as well as alcoholic liver disease (*3–5*). While analytical methods to identify reactive metabolites and their protein binding potencies in vitro are now routinely used in drug development to eliminate potentially toxic candidates, the ability to extend in vitro studies to in vivo toxicity is limited (*6–8*). Reactive intermediates modify a number of common abundant proteins, and there appears to be no single modified protein solely responsible for the toxic response. Thus, characterization of the entire spectrum of modified proteins is an important step in understanding mechanisms of toxicity.

A number of proteins adducted by reactive metabolites of drugs and xenobiotics, as well as endogenous reactive products, such as acetaminophen (APAP), bromobenzene (BB), and 4-HNE, have been identified from intact animals (*3, 4, 9–22*). Detection of adducted proteins was accomplished by the use of radioactively labeled toxicants or by employing adduct-specific antibodies for immunoblotting. These approaches are limited by sensitivity in the case of radiochemical detection or by specificity in the case of adduct-specific antibodies. These limitations preclude detection of the complete profile of adducts.

Our laboratory is interested in the chemistry and biology of teucrin A, a major constituent of the *neo*-clerodane diterpenoid fraction of the hydroalcoholic extract of germander (*Teucrium chamaedrys*). Germander has been used to treat obesity and is a flavoring agent in alcoholic beverages (Scheme 1) (*23, 24*). Oral administration of teucrin A or germander extracts causes depletion of intracellular glutathione and damage to cellular protein thiols, resulting in elevated plasma ALT activity and significant centrilobular liver injury in mice (*25, 26*). Isolated diterpenoid fractions from germander cause apoptosis in isolated rat hepatocytes (*27*). The toxicity of teucrin A in

* To whom correspondence should be addressed. Tel: 615-343-7329. Fax: 615-343-7534. E-mail: larry.marnett@vanderbilt.edu.
† Department of Biochemistry.
‡ Department of Chemistry.
§ Department of Pharmacology.
|| Mass Spectrometry Research Center.

10.1021/tx7001405 CCC: $37.00
Published on Web 09/25/2007

Scheme 1. Proposed Mechanism for the Bioactivation of 3-Substituted Furans and the Formation of Reactive Electrophilic Enedial Metabolites

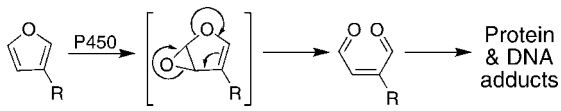

Scheme 2. Synthesis of the Enedial Derivative of Teucrin A and N-Terminal Biotinylated Peptide Conjugates[a]

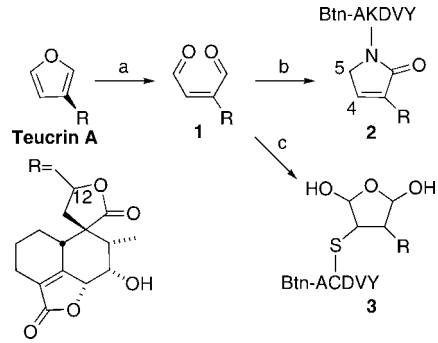

[a] (a) Dimethyldioxirane (DMDO), acetone. (b) Btn-AKDVY, 0.1 M phosphate buffer, pH 7.4. (c) Btn-ACDVY, 0.2 M phosphate buffer, pH 7.4.

mice has been attributed to metabolic activation of the 3-substituted furan ring to an electrophilic metabolite (*25*). This hypothesis is supported by the observation that a tetrahydrofuran analogue is not toxic (*25*). By analogy to other furan-containing compounds, such as methylfuran, furosemide, 4-ipomeanol, menthofuran, and aflatoxin (*28–35*), 1,4-enedials or possible epoxide precursors are the likely reactive metabolites (Scheme 2) (*34–37*).

Previously, we reported the synthesis of the enedial derivative of teucrin A (**1**) and the structural characterization of its conjugates with *N*-acetyl lysine methyl ester (NAL) and *N*-acetyl cysteine (NAC). In addition, we prepared conjugates of **1** to the lysine-containing peptides, RKDVY and N-terminal biotinylated RKVDY (*38*). The ability to efficiently synthesize stable peptide adducts of **1** provided a tool for the development of selective antibodies against the teucrin epitope (*39*). Adducted peptides were used to screen a phage-displayed single-chain antibody library for single-chain fragment variables (ScFvs) that recognize the teucrin-adducted peptides independently of the sequence of the peptide. Candidates ScFvs were further screened to identify ScFvs that detect adducted proteins by Western blotting and that immunoprecipitate them. These antibodies were used to validate the production of teucrin–protein adducts in vivo and to enrich them for mass spectrometric analysis. We report here a comprehensive set of protein targets of activated teucrin A. We also describe the possible consequences of modification based on network analysis of the modified proteins.

Materials and Methods

Reagents and Solvents. HPLC grade solvents for column chromatography and HPLC were obtained from Fisher (Pittsburg, PA) and were used as received. Reagent grade chemicals were obtained from Aldrich (Milwaukee, WI). Biocytin [Ser^{25}] protein kinase C fragment 19–31 and KKRAARATS amide were purchased from Sigma-Aldrich (St. Louis, MO). 5-mer peptides were purchased from Sigma-Genosys (The Woodlands, TX). Thin-layer chromatography was performed on silica gel GF glass plates from Analtech (Newark, DE). The chromatograms were visualized under UV (254 nm), fluorescence, or by staining with sulfuric acid solution, followed by heating. Column chromatography was performed using silica gel 60–100 mesh from Fischer. Teucrin A was a generous gift from Dr. Corrado Galli, University of Milan (Italy). Purification and characterization of teucrin A were performed as described previously (*38*). DMDO was prepared as previously reported (*38, 40*).

Instrumental Analysis. UV spectra were recorded using a Hewlett-Packard UV/vis model 89500 spectrometer. Mass spectra were recorded on a Finnigan TSQ 7000 triple-quadrupole spectrometer under positive or negative ion mode. ^{1}H NMR spectra were recorded on a Bruker 300, 400, and 500 MHz NMR spectrometers using acetone-d_6 and DMSO-d_6 as solvent and internal standard. HPLC analysis was performed on Waters 1525 Binary HPLC Pump with Waters 2996 Photodiode Array Detector on the reversed phase Jupiter C18 5 μm 250 mm $\times$ 4.6 mm or 150 mm $\times$ 4.6 mm column at 1 mL/min (Phenomenex, CA). Semi-preparative HPLC was performed using Jupiter C18 5 μm 250 mm $\times$ 10 mm column at 4 mL/min.

Enedial derivative of teucrin A (**1**) was prepared and characterized as previously reported (*38*). Teucrin A (10 mg, 0.029 mmol) was dissolved in 0.5 mL of anhydrous acetone-d_6, and the solution was cooled in the acetone/dry ice bath. Cold DMDO-d_6 (1.2 mL, 0.034 mmol) was added under argon atmosphere. The reaction mixture was allowed to warm up to room temperature, and the progress of the reaction was monitored by ^{1}H NMR. The reaction was complete in 2 h. Upon disappearance of the starting material, nitrogen was blown through the solution to eliminate unreacted DMDO-d_6, and the product was stored as acetone-d_6 solution at -20 °C.

Synthesis of Teucrin A-Adducted Biotinylated Peptides. Btn-AKDVY (2 mg, 2.14 μmol) and Btn-ACDVY (2 mg, 2.20 μmol) were dissolved in 0.2 mL of 0.2 M sodium phosphate buffer, pH 7.4. The acetone solution of **1** (1 equiv, 26 mM) was added, and mixtures were incubated at 37 °C. The reactions were monitored by HPLC/UV looking at the disappearance of the starting peptides. Adducted products were purified by HPLC and analyzed by LC-MS/MS. Liquid chromatography was performed using a gradient at 1 mL/min as follows: from 0 to 1 min, hold 100% A; from 1 to 20 min, linear gradient to 50% A; and from 20 to 25 min, linear gradient to 100% A, where A = water + 0.1% acetic acid and B = acetonitrile + 0.1% acetic acid.

Phage Antibody Selection on Teucrin A Dial-Btn-AKDVY. A rodent phage displayed recombinant antibody library ($\sim$2.9 $\times$ 10^9 members) was generated according to a previously described protocol (*41*) with minor modifications. The library was used to obtain teucrin A-specific ScFv antibodies. ScFv antibodies stemming from the library bear an E-tag peptide sequence. E-tagged ScFv antibodies bound to antigen can be detected using the an anti-E tag monoclonal antibody conjugated to peroxidase (Anti-E/HRP, G. E. Healthcare catalog no. 27941301) and purified from *Escherichia coli* using an anti-E tag monoclonal antibody column (G. E. Healthcare catalog no. 17-1362-01). For phage antibody selections, Nunc Maxisorb Immunotubes were coated with 1 mL of streptavidin diluted to 5 μg/mL in phosphate-buffered saline (PBS) for 1 h at room temperature (RT) and then blocked with PBS containing 0.1% Tween 20 (PBS-T) for 1 h at RT.

One milliliter of teucrin A-adducted Btn-AKDVY diluted to 1 μg/mL PBS-T was added to streptavidin-coated tubes. The tubes were incubated for 1 h at RT, then washed six times (10 seconds per wash) with PBS-T to remove unbound teucrin A-adducted Btn-AKDVY. The phage-displayed antibody library was diluted to 10^{12} phage per mL in PBS-T and incubated for 2 h at RT to block nonspecific phage-antibody binding activity. One milliliter of phage antibody library in PBS-T was added to teucrin A-adducted Btn-AKDVY on streptavidin-coated tubes. After a 2 h incubation at RT, the tubes were washed six times (10 seconds per wash) with PBS-T to remove unbound phage antibodies. After the first round of selection, phage-displayed antibodies, bound to teucrin A-adducted Btn-AKDVY on streptavidin-coated tubes, were eluted with 1 mL of 100 mM triethylamine for 10 min at RT. The pH of the eluted phage antibodies, in triethylamine, was adjusted to a pH of 7–8 with 0.5 mL of 1 M Tris, pH 7.4–8.

The phage antibodies were then used to infect log phase *E. coli* TG1 cells, incubated at 37 °C for 1 h. Infected *E. coli* TG1 cells were plated onto 2xYT AG agar plates (17 g of Bacto-tryptone, 10 g of Bacto-yeast extract, 5 g of NaCl, 20 g of glucose, 100 mg of ampicillin, and 15 g agar per liter, final concentration), incubated overnight at 30 °C, and helper phages were rescued with M13KO7 to produce phage-displayed antibodies, in bacterial culture supernatant, for use in a second round of phage antibody selection according to methods described previously (*42*). One microliter of Tween 20 was added to 1 mL of phage-displayed antibodies in bacterial culture supernatant to block nonspecific phage-antibody binding activity. After a 2 h incubation at RT, the blocked phage-displayed antibodies were used for a second round of selection on teucrin A-adducted Btn-AKDVY on streptavidin-coated tubes. The protocols used to carry out the first round of phage antibody selection were also used to perform the second round of selection.

The protocols used to identify antigen-specific ScFv by an enzyme-linked immunsorbant assay (ELISA) and to grow and purify ScFv have been described (*42*) and modified as follows to obtain teucrin A-specific ScFv. Briefly, bacterial colonies stemming from the second round of phage antibody selection were picked from 2xYT AG agar plates into 384 well microtiter plates containing 2xYT AI (17 g of Bacto-tryptone, 10 g of Bacto-yeast extract, 5 g of NaCl, 100 mg of ampicillin, and 1 mM IPTG, final concentration) and induced to express soluble ScFv recombinant antibodies. For ELISA, Nunc 384 well microtiter plates were coated with streptavidin (5 μg/mL PBS, 25 μL/well) for 1 h at RT and then blocked with PBS-T. Teucrin A-adducted Btn-AKDVY or ACDVY (positive control) or Btn-AKDVY or ACDVY (negative control) diluted to 1 μg/mL PBS-T, 25 μL/well was then added to microtiter wells. After a 1 h at RT incubation, plates were washed six times with PBS-T (10 seconds per wash), emptied, and then used for assay as described (*42*). Bacterial colonies expressing ScFv reactive by ELISA with the positive but not negative control were subsequently identified and used to produce teucrin A-specific ScFv.

Teucrin A Treatment of Rats. Animal protocols were performed under the approval of Vanderbilt University and in accordance with the Institutional Animal Care and Use Committee policies. Male Sprague Dawley rats (225–250 g) with vascular catheters surgically implanted in the femoral and jugular veins were obtained from Charles River Laboratories (Wilmington, MA). The rats were allowed to feed a standard diet for 48 h ad libitum and were starved overnight prior to the experiment. Animals, in triplicate, were dosed orally by gavage a single dose of teucrin A at 25 mg/animal (100 mg/kg bw) in minimum DMSO in corn oil or DMSO in corn oil alone (total volume, 1 mL). The plasma levels of alanine amino transferase (ALT) were monitored over time (0.4 mL blood samples were taken at 0, 1, 3, 6, 10 and 24 h) using ALT Colorimetric Assay Kit (Teco Diagnostics, Anaheim, CA). The animals were sacrificed 24 h after the dose, and the livers were excised. Liver homogenate was separated into cytosolic and particulate protein and analyzed by Western blotting for teucrin A adducts using teucrin A-specific ScFv monoclonal antibodies as described below.

Rat Liver Homogenization and Fractionation. Thawed livers were weighed and finely scissor-minced with a scalpel. The tissue was transferred into a 50 mL Potter–Elvehjem glass container, 20 mL of ice cold homogenization buffer (20 mM Tris-HCl, pH 8.0, and 250 mM sucrose, containing 1 tablet of Roche protease inhibitor mix) was added, and the livers were homogenized. The mixtures were centrifuged at 250*g* for 15 min at 4 °C, and the supernatant was collected. The pellet was rehomogenized in an equal volume of homogenization buffer and centrifuged. Combined supernatants (homogenates) were centrifuged at 184000*g* for 50 min at 4 °C. The supernatant was collected as a cytosolic fraction. The pellet was resuspended in homogenization buffer and centrifuged at 184000*g* for 50 min at 4 °C. The supernatant was discarded, and the pellet was resuspended in 20 mM Tris-HCl, pH 8.0, as a particulate. The particulate was then incubated for 20 min on ice in the buffer containg 0.1% Triton X-100 and centrifuged at 184000*g* for 50 min at 4 °C, and the resulting supernatant was collected as solubilized protein from particulate (membrane proteins). Cytosolic fractions were desalted on a Sephadex G25 resin with 20 mM Tris-Hcl, pH 8.0, at 4 °C. Protein concentrations were determined by BCA assay (Pierce).

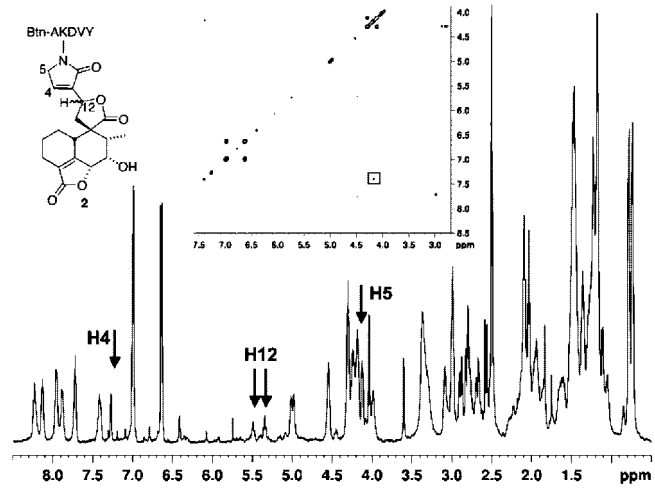

Figure 1. ^{1}H NMR and COSY spectra (500 MHz, DMSO-d_6) of the conjugate of **1** with Btn-AKDVY peptide (**2**) with the labeled structure showing the positions of the relevant protons.

Western Analysis Using 2I2 ScFv Antibody. Protein samples were separated on 10% SDS-PA gels and transferred to nitrocellulose membranes (Biorad). The membranes were blocked in 5% nonfat dry milk in PBS for 1 h at RT on a rotary shaker. Blocked membranes were transferred into a solution of primary ScFv antibody and anti-E/HRP secondary antibody diluted 1:20000 in 5% nonfat dry milk/PBS and incubated for 1 h at RT, subsequently washed with DI water, and incubated in 5% nonfat dry milk/PBS/0.1% Tween 20 for 1 h (the solution was changed at least two times during this period). Membranes were washed again in DI water, the ECL substrate solution (Pierce no. 34077) was applied for 5 min at RT, and the excess solution was dried with filter paper. The membranes were placed in the cassette, and the film was exposed for 3–60 s and developed.

Anti-E Sepharose Bead Preparation. NHS-activated Sepharose beads (G. E. Healthcare catalog no. 17-0906-01) were washed with 10 volumes of cold 1 mM HCl, suspended in 2 mL of PBS, and incubated with 1 mg of anti-E tag monoclonal antibody (G. E. Healthcare catalog no. 27-9412-01) at 18 °C for 4 h, followed by the addition of 4 mL of 110 mM Tris-HCl, 10 mM ethanolamine, pH 7.4, and was allowed to react at 18 °C for 3 h. The beads were washed in three cycles alternating 3× column volume of 100 mM Tris-HCl, pH 8.0, and 3× column volume of 100 mM ammonium formate, pH 4.0. Finally, the beads were washed 3× column volume of water and stored in 1.5 mL of 25% ethanol at 4 °C.

2I2 ScFv Immunoprecipitation of Teucrin A Enedial-Adducted BSA. The 2I2 ScFv antibody was affinity-purified from the periplasmic extracts of *E. coli* using an anti-E tag monoclonal antibody column (G. E. Healthcare catalog no. 17-1362-01). Anti-E tag Sepharose beads (20 μL) were transferred on a mini-spin column (Biorad) and washed 3 × 200 μL of PBS-T. Then, 60 μL of PBS-T was added, followed by 15 μL of 2I2 ScFv (0.23 mg/mL) and 200 μL of teucrin A enedial-adducted BSA or control BSA (2 mg protein/mL). The mixtures were incubated for 1 h at RT. To wash off unbound and nonspecifically bound proteins, the beads were washed 5 × 50 μL of PBS-T, followed by 3 × 50 μL of PBS and and 3 × 50 μL of water. Proteins retained on the beads were sequentially eluted with 1 M sodium chloride (50 μL) and increasing concentrations of acetonitrile (5, 20, and 50%, 50 μL each) and, finally, 50 μL of 50% ACN/1% formic acid. Sodium chloride eluates were desalted using a protein desalting columns (Biorad). Fractions containing formic acid were neutralized with 5 M NaOH. All fractions were then supplemented with 5× Laemmli buffer and heated for 10 min at 95 °C, and 10 μL of each sample was loaded on 12% Tris-Gly gel (Invitrogen). Proteins were separated using SDS Tris-Gly running buffer (Invitrogen) at 140 V for 85 min and

Scheme 3. Proposed Mechanism of Pyrroline-2-one Adduct Formation and Epimerization of C12

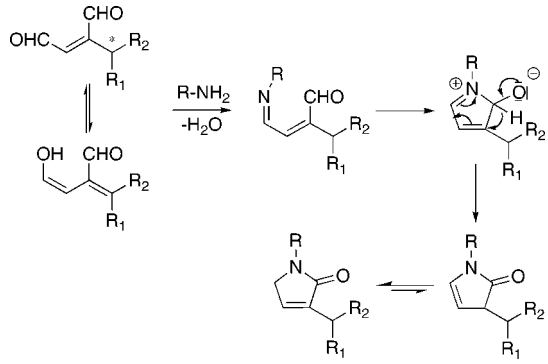

visualized by Coomassie Blue staining (Colloidal Blue from Invitrogen). Protein-containing bands were excised and in-gel digested with trypsin. Resulting peptide mixtures were analyzed by LC-MS/MS.

2I2 ScFv Immunoprecipitation of Rat Liver Membrane Fractions (RLM). Anti-E tag Sepharose beads (30 μL) were transferred on a mini-spin column (Biorad) and washed 3 × 200 μL of PBS/0.1% Tween 20. Then, 80 μL of PBS-T was added, followed by 20 μL of 2I2 ScFv (0.23 mg/mL) and 200 μL of solubilized rat liver membrane fractions (3 mg protein/mL). The mixtures were incubated on a shaker for 2 h at 18 °C, followed by washing with PBS/Tween 20, PBS, and water. The proteins were eluted from the beads using 2× Laemmli buffer and heated at 95 °C for 10 min. The samples were cleaned up on 12% Tris-Gly gel (Invitrogen) using Tris-Gly SDS running buffer before enzymatic digestion and mass spectral analyses.

2I2 ScFv Immunoprecipitation of Rat Liver Cytosolic Fractions (RLC). Anti-E tag Sepharose beads (30 μL) were transferred on a mini-spin column (Biorad), washed 3 × 200 μL of PBS-T, and resuspended in 30 μL of PBS-T. A random nonspecific ScFv was added (30 μL, 0.33 mg/mL), followed by 200 μL of RLC (3 mg protein/mL). The mixtures were incubated for 1 h at ambient temperature. The supernatant was collected (15 μL was collected for Western blot analysis) and transferred into a vial containing a fresh mix of washed anti-E beads (100 μL) and anti-teucrin A-specific 2I2 antibody (90 μL, 0.23 mg/mL). The mixtures were incubated at ambient temperature for 1 h (or 4 °C overnight), followed by a washing procedure after collecting the supernatant as follows: (i) 100 μL of PBS-T, 15 min; (ii) 100 μL of PBS, 10 min; (iii) 100 μL of water; (iv) 2 × 100 μL of 1 M NaCl, 15 min; (v) 5–50% aqueous acetonitrile gradient, 100 μL fraction/15 min each; and (vi) 100 μL of 50% aqueous acetonitrile/0.1%formic acid. Sodium chloride eluates were desalted using protein desalting columns (Biorad). Fractions containing formic acid were neutralized with 5 M NaOH. All fractions were then supplemented with 5× Laemmli buffer and heated for 10 min at 95 °C, and 10 μL of each sample was loaded on 12% Tris-Gly gel (Invitrogen). Proteins were separated using SDS Tris-Gly running buffer (Invitrogen) at 140 V for 85 min and visualized by Coomassie Blue staining (Colloidal Blue from Invitrogen) or by silver staining (kit from Amersham Biosciences) or transferred onto a nitrocellulose membrane (Biorad) for Western blotting.

In-Gel Digestion and LC-MS/MS Analysis. Protein samples were run either just 1.5 cm into a 10% SDS-PAGE gel (for rat samples) to clean up the samples from residual detergents and salts as previously described (*43*) or fully into the gel, and specific protein bands were excised. Protein bands were cut out from gels and in-gel digested with trypsin or chymotrypsin as previously described (*44*). LC-MS analysis of the resulting peptides was performed using a Thermo LTQ ion trap mass spectrometer equipped with a Thermo MicroAS autosampler and Thermo Surveyor HPLC pump, nanospray source, and Xcalibur 1.4 instrument control. The peptides were separated on a packed capillary tip, 100 μm × 11 cm, with C_{18} resin (Jupiter C_{18}, 5 μm, 300 Å; Phenomonex, Torrance, CA)

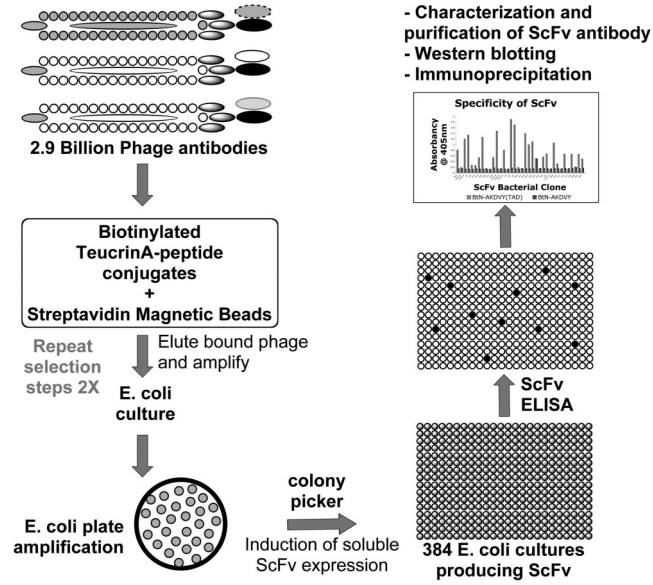

Figure 2. Process of the anti-teucrin A ScFv antibody selection from the rodent phage-displayed library.

using an inline solid phase extraction column that was 100 μm × 6 cm packed with the same C18 resin [using a frit generated from liquid silicate Kasil 1 (*45*) similar to that previously described (*46*), except the flow from the HPLC pump, which was split prior to the injection valve]. The flow rate during the solid-phase extraction phase of the gradient was 1 μL/min, and during the separation phase, it was 700 nL/min. Mobile phase A was 0.1% formic acid, and mobile phase B was acetonitrile with 0.1% formic acid. A 95 min gradient was performed with a 15 min washing period (100% A for the first 10 min followed by a gradient to 98% A at 15 min) to allow for solid-phase extraction and removal on any residual salts. After the initial washing period, a 60 min gradient was performed where the first 35 min was a slow, linear gradient from 98 to 75% A, followed by a faster gradient to 10% A at 65 min, and an isocratic phase at 10% A to 75 min. MS/MS scans were acquired using an isolation width of 2 *m/z*, an activation time of 30 ms, an activation Q of 0.250, and 30% normalized collision energy using one microscan and a maximum injection time of 100 for each scan. The mass spectrometer was tuned prior to analysis using the synthetic peptide TpepK (AVAGKAGAR). Typical tune parameters were as follows: spray voltage of between 1.8 kV, a capillary temperature of 150 °C, a capillary voltage of 50 V, and tube lens of 100 V. The MS/MS spectra of the peptides were acquired using data-dependent scanning, in which one full MS spectrum was followed by three MS/MS spectra.

Database Searching and Data Analysis. The "ScanDenser" algorithm read tandem mass spectra stored as centroided peak lists from Thermo RAW files and transcoded them to DTA files. Spectra that contained fewer than 26 peaks or that had less than 2e1 measured TIC did not result in DTAs. DTAs from singly charged spectra were created if 90% of the TIC occurred below the precursor ion; all other spectra were processed as both doubly and triply charged DTAs. Proteins were identified using the TurboSEQUEST version 27 (revision 12) algorithm (Thermo Electron, San Jose, CA) (*47*) on a high-speed, multiprocessor Linux cluster in the Advanced Computing Center for Research & Education at Vanderbilt University, using the Sequest algorithm using either the rat or the bovine subset of the Uniref100 database. The databases were reversed so that false discovery rates could be determined, and the reversed version of each protein sequence was appended to the forward database for a total of 108994 and 112404 sequences in the rat and bovine databases, respectively. The false discovery rates were calculated as previously described (*48*). Differential modifications for carbamidomethylation of cysteines and oxidation of methionines as well as teucrin A adducts with a mass shift of 342 on lysines and 342 and 376 on cysteines were allowed with

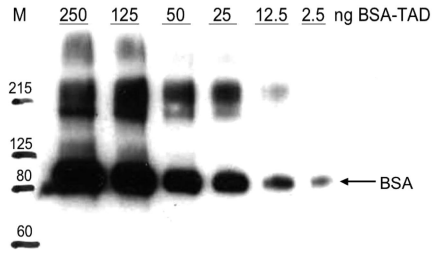

Figure 3. Western blot of BSA adducted in vitro with teucrin A enedial using the periplasmic extracts of the selected 2I2 ScFv clone.

peptide and fragment ion tolerances of 2.5 and 1.0 Da, respectively. Up to 10 missed cleavages and only fully tryptic peptides were allowed. Protein matches were preliminarily filtered using the following criteria: if the charge state of the peptide is 1, the Xcorr is greater than or equal to 1, the RSp is less than or equal to 5, and the Sp is greater than or equal to 350; if the charge state is 2, the Xcorr is greater than or equal to 1.8, the RSp is less than or equal to 5, and the Sp is greater than or equal to 350; and if the charge state is 3, the Xcorr is greater than or equal to 2.5, the RSp is less than or equal to 5, and the Sp is greater than or equal to 350. Once filtered based on these scores, all protein matches that had less than two peptide matches were eliminated from the search.

Network Generation and Functional Analysis Using Ingenuity Pathways Analysis. The networks and functional analyses were generated through the use of Ingenuity Pathways Analysis (Ingenuity Systems, www.ingenuity.com). A data set containing gene identifiers and corresponding expression values was uploaded into the application. Each gene identifier was mapped to its corresponding gene object in the Ingenuity Pathways Knowledge Base. These genes, called Focus Genes, were overlaid onto a global molecular network developed from information contained in the Ingenuity Pathways Knowledge Base. Networks of these Focus Genes were then algorithmically generated based on their connectivity. The Functional Analysis of a network identified the biological functions and/or diseases that were most significant to the genes in the network. The network genes associated with biological functions and/or diseases in the Ingenuity Pathways Knowledge Base were considered for the analysis. Fischer's exact test was used to calculate a *p* value determining the probability that each biological function and/or disease assigned to that network is due to chance alone. Canonical pathways analysis identified the pathways from the Ingenuity Pathways Analysis library of canonical pathways that were most significant to the data set. The significance of the association between the data set and the canonical pathway was measured in two ways: (i) A ratio of the number of genes from the data set that map to the pathway divided by the total number of genes that map to the canonical pathway is displayed, and (ii) Fischer's exact test was used to calculate a *p* value determining the probability that the association between the genes in the data set and the canonical pathway is explained by chance alone. A network is a graphical representation of the molecular relationships between genes/gene products. Genes or gene products are represented as nodes, and the biological relationship between two nodes is represented as an edge (line). All edges are supported by at least one reference from the literature, from a textbook, or from canonical information stored in the Ingenuity Pathways Knowledge Base. Human, mouse, and rat orthologues of a gene are stored as separate objects in the Ingenuity Pathways Knowledge Base but are represented as a single node in the network. Nodes are displayed using various shapes that represent the functional class of the gene product. Edges are displayed with various labels that describe the nature of the relationship between the nodes (e.g., P for phosphorylation and T for transcription).

Results

Synthesis of Biotinylated Peptides Containing a Teucrin A Epitope. To generate an anti-teucrin A adduct-specific antibody, a hapten containing an appropriate epitope was designed, synthesized, and structurally characterized. First, teucrin A was oxidized with DMDO affording **1** (Scheme 2), as previously described (*38*). N-terminal biotinylated peptide AKDVY was reacted with **1** in phosphate buffer, pH 7.4, at 37 °C overnight. The reaction products were isolated by HPLC and characterized by mass spectrometry. The major HPLC peak eluting at 21.8 min exhibited a base peak at *m/z* 639.0, corresponding to the $[M + 2H]^{2+}$, and a molecular ion at *m/z* 1277.0, representing the $[M + H]^{+}$. The observed masses matched the predicted formation of the anticipated pyrroline-2-one product. Because there are two possible regioisomers of the pyrroline-2-one ring that can be formed in this reaction, specifically three- or four-substituted pyrrolinones, ^{1}H NMR and COSY spectra of the HPLC purified conjugate were measured and examined for the presence of signals characteristic of the two regioisomers (*38, 49*). A signal observed at 7.3 ppm corresponded to the H4 proton of the three-substituted pyrroline-2-one **2**, as described for the conjugate of **1** with NAL (Figure 1) (*38*). A cross-peak in the COSY spectrum between the signal at 7.3 ppm and a signal at 4.2 ppm, which is consistent with the reported value for the methylene group protons H5 of the three-substituted pyrrolinone ring, confirmed the structural assignment. Two triplet signals at 5.34 and 5.49 ppm were assigned to H12 of the teucrin A moiety. Previously, we reported evidence for an equilibrium between the enedial and the hydroxyenal tautomers in aqueous environments, resulting in epimerization of the H12 proton of **1** and formation of diastereomeric products in the reactions of **1** with NAL or NAC. This is consistent with the observation of two triplets for the H12 proton (Scheme 3) (*38*).

To obtain an ScFv antibody useful for the investigation of proteins adducted with activated teucrin A in vivo, the selection was designed so that the antibody would recognize not only lysine but potential cysteine conjugates as well; thus, its recognition would be independent of adduct structure or peptide sequence. For this purpose, N-terminal biotinylated peptide, ACDVY, was reacted with **1** under the same conditions as described above for the Lys-containing protein. The reaction afforded one major product, which was isolated by HPLC and characterized by mass spectrometry. The *m/z* of the base peak of the isolated material was 1307.65, corresponding to the $[M + Na]^{+}$ of the hydrated cyclic Michael adduct **3** and the *m/z* of the molecular ion $[M + H]^{+}$ was 1285.56. We previously showed that hydrated adducts of NAC with **1** are unstable to extensive purification (*38*) so the Btn-ACDVY peptide conjugates were not characterized by NMR.

Table 1. Residues Adducted in BSA by 1 in Vitro[a]

residue no.	peptides detected*
K374 (351), K568 (545)	≥10
K36 (12), K138 (R114), K160 (136), K204 (181), K304 (281)	5–7
K28, K100, K412, K420, K455, K463, 489	4
K140, K235, K248, K251, K256, K266, K346, K548	3
K75, K88, K117, K183, K245, K263, K285, K297, K299, K399, K401, K437, K489, K547, K561	<2
C58	2

[a] The asterisk shows the number of times that the peptides with adducted residues were detected in three independent analyses. Numbers in parentheses are the corresponding residues in the crystal stucture of HSA. The complete MS data are available in the Supporting Information (Table S1b and MS/MS figures).

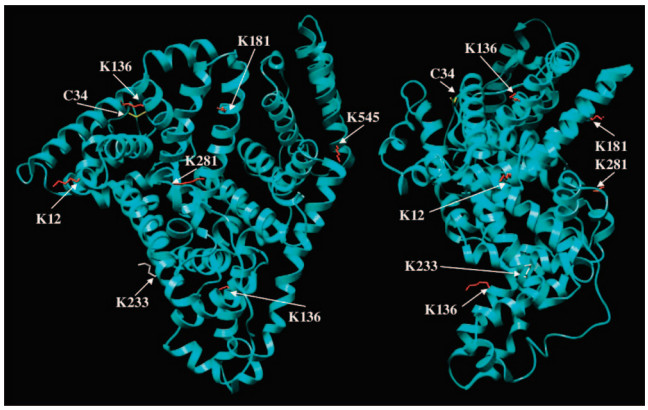

Figure 4. Crystal structure of human serum albumin (PDB: 1AO6) with the highlighted residues corresponding to the ones significantly adducted in bovine serum albumin (BSA) by teucrin A enedial **1** in vitro (lysines in red, cysteine in yellow, and L233 in white). The right frame is rotated 90° with respect to the left frame.

Selection of a Teucrin A-Specific ScFv Antibody. To obtain a tool to study teucrin A-adducted proteins in vitro and in vivo, a monoclonal ScFv antibody was isolated and characterized from a rodent phage-displayed library (Figure 2). The purified teucrin A enedial-peptide conjugate with biotinylated AKDVY peptide **2** was used as an antigen for two rounds of phage antibody selection. An ELISA was used to detect teucrin A-specific ScFv. Thirty-two ScFv antibodies interacted strongly with teucrin A-adducted Btn-AKDVY peptide conjugate and weakly with unmodified Btn-AKDVY peptide. These ScFvs were further screened against the purified teucrin A-peptide conjugate with the biotinylated cysteine-containing ACDVY peptide, **3**, and positive clones were selected based on their ability to recognize both lysine and cysteine conjugates equally well (Figures S1 and S2, Supporting Information). Four ScFv clones (2E18, 2F7, 2I2, and 2G7) were further characterized by screening against synthesized teucrin A enedial-peptide conjugates that contained variable amino acid sequences (RKVDY, Btn-RKDVY, biocytin [Ser^{25}] protein kinase C fragment 19–31, and KKRAARATS amide) to ensure that the ScFv antibodies were teucrin A-specific and not teucrin A-amino acid sequence-specific.

Western Blotting with an Anti-Teucrin A ScFv Antibody Using Teucrin A Enedial-Adducted BSA. Western blotting and immunoprecipitation procedures with the ScFv antibody (designated 2I2) were developed to detect and enrich teucrin A-adducted proteins from complex protein mixtures. Four other teucrin-specific ScFv were also characterized for use in Western blot. For Western blot protocol optimization purposes, bovine serum albumin (BSA) was chosen as a representative protein and reacted with two equivalents of **1** at 37°C overnight in phosphate buffer pH 7.4 to generate a teucrin A-adducted BSA standard. As a control, BSA was incubated under the same conditions in the absence of **1**. For Western blot analysis, 50 μg of teucrin A-adducted or control BSA were resolved by SDS polyacrylamide gel electrophoresis using a single-well pre-cast prep gel. Proteins were transferred to nitrocellulose and Western blot analysis was performed using ScFv in *E. coli* periplasmic cell extracts. E-tagged ScFv bound to teucrin A-adducted BSA on nitrocellulose was visualized using an Anti-E/HRP conjugate, an HRP-chemiluminescent substrate film. *E. coli* periplasmic extract containing unpurified 2I2 could be diluted 1:20:000 for use in Western blot and exhibited the highest affinity for the adducted BSA and the lowest background of the four clones tested (Figure S3, Supporting Information). The 2I2 ScFv specifically detected protein bands in lanes where adducted BSA was loaded, whereas

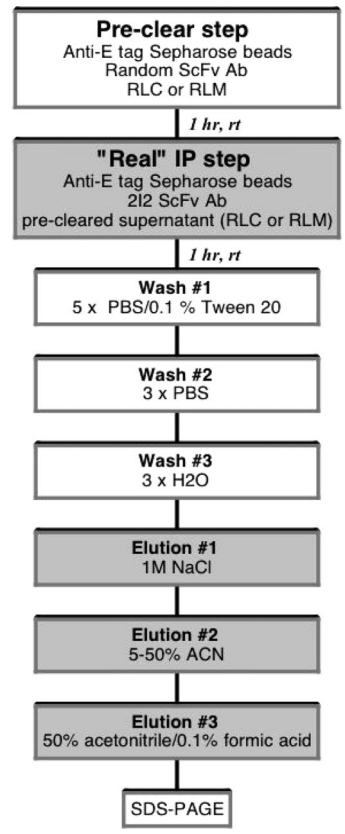

Figure 5. Flow chart of the immunoprecipitation procedure with the 2I2 ScFv antibody.

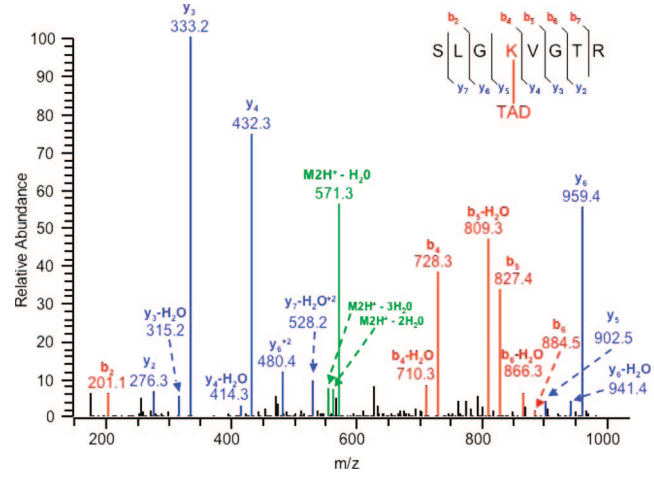

Figure 6. Representative MS/MS spectrum of a BSA peptide modified on the lysine residue by teucrin A enedial.

there was no detectable signal in lanes loaded with control BSA. The 2I2 ScFv detected 2.5 ng of the adducted BSA in Western blots using a film exposure time of ten seconds or less (Figure 3). The immunoreactive high molecular weight bands (>200 kDa) in the Western blot analysis resulted from adduction of protein contaminants in the purchased BSA as shown by Colloidal Blue staining and confirmed by LC-MS/MS (Figure S3 and Table S1, Supporting Information).

To confirm the modifications caused by **1** on the BSA protein, the adducted sample was subjected to LC-MS/MS analysis. First, the protein sample was purified by SDS polyacrylamide gel electrophoresis and stained with Colloidal Blue. The protein band corresponding to the adducted BSA was excised and in-gel digested with trypsin. LC-MS/MS analysis of the trypsin digest revealed numerous lysines modified by **1**. The increases

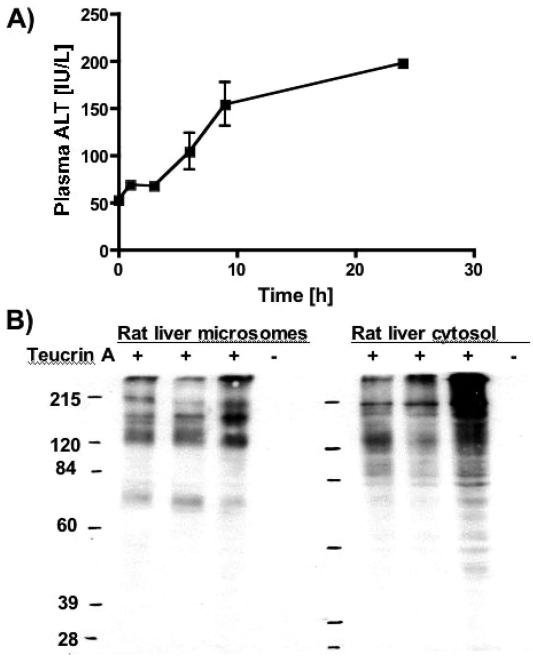

Figure 7. (A) Time course of the plasma alanine aminotrasferase (ALT) activity in Spague–Dawley rats ($n = 3$) after oral administration of 100 mg/kg of teucrin A. (B) Western blot of the rat liver proteins adducted in vivo by teucrin A metabolite(s) detected with the periplasmic extracts of the selected 2I2 ScFv clone.

in molecular weight of the modified peptides that were observed corresponded to the formation of the pyrroline-2-one between the lysine residues and **1** as described above for the peptide conjugates. A single cysteine residue (C56) was covalently modified, resulting in the formation of the conjugate **3**. The residues that were found adducted in BSA are listed in Table 1. Several lysine-modified peptides were detected numerous times in repeated analyses, possibly due to preferential adduction by the electrophile. The residues detected five or more times were mapped onto the crystal structure of human serum albumin (HSA) (Figure 4) (*50*). The residues copiously modified were distributed throughout the HSA structure and most of the adducted residues were in solvent accessible regions. The detailed kinetics and reactivity studies were not performed.

Immunoprecipitation of Teucrin A Enedial-Adducted BSA Using 2I2 ScFv. To ensure that the 2I2 ScFv antibody was capable of enriching the teucrin A-adducted proteins, immunoprecipitation was performed with BSA adducted with **1** and unadducted BSA using the 2I2 ScFv antibody. Sepharose beads covalently cross-linked with anti-E tag IgG antibody, the affinity-purified 2I2 ScFv antibody and adducted or control BSA were incubated as described in Materials and Methods. An optimized procedure for the selective elution of the bound proteins is illustrated in Figure 5. 1M Sodium chloride was found to selectively elute adducted BSA bound to the beads without disrupting the ScFv-anti-E tag bindings. Further washes with increasing concentrations of acetonitrile (from 5 to 50%) and the addition of formic acid (1%) eluted the residual adducted BSA. The final acidic wash also released the ScFv from the beads. Minimal non-specific protein binding was observed in the control BSA immunoprecipitation by Colloidal blue as well as silver staining. In LC-MS/MS analysis, the enrichment of the BSA peptides in the samples treated with **1** over the control in the sodium chloride elution fraction was consistently over fourfold. In addition, nine modified peptides were identified in the sodium chloride elution fraction, all of which were abundantly present in the tryptic digest of the adducted BSA without immunoprecipitation, including the peptide shown in Figure 6. Thus, the enrichment procedure consisting of the selective elution of adducted protein with sodium chloride and gradient elution of bound protein with increasing concentrations of acetonitrile appeared to give satisfactory results and was further used to immunoprecipitate proteins adducted with activated teucrin A *in vivo* in rat liver. False discovery rates in these experiments were 1% or less.

Identification of Teucrin A Protein Adducts in Vivo by Western Blot Analysis. In order to generate a toxic response *in vivo*, we needed to determine an optimal dose of teucrin A in rodents. Previous studies found that the hydroalcoholic extract of *T. chamaedrys* was generally well-tolerated by male Sprague-Dawley rats up to 13 weeks at 56 mg/kg/day administered orally (teucrin A equivalent of 0.4 mg/kg/day) (*23*). Chronic exposure of rats to approximately 2 mg/kg/day of teucrin A over 13 weeks lead to significant changes in the liver, mainly hepatocellular hypertrophy and steatosis (*23*). A higher chronic dose of 10 mg/kg/day of teucrin A was poorly tolerated (*23*). Subchronic four week dosing of 10 mg/kg/day caused liver modifications of degenerative origin and necrosis of isolated rat hepatocytes (*23*). A single intragastric administration of a germander tea lyophilisate (1250 mg/kg) or the furan neoclerodane diterpenoid fraction (125 mg/kg) produced similar mid-zonal liver cell necrosis at 24 hours in mice (*51*). In another *in vivo* study, a single oral administration of an ethanolic extract of germander (2000–4000 mg/kg) to mice caused increases in plasma alanine aminotransferase (ALT) activity and mid-zonal hepatic necrosis 24 hours after dosing (*25*). A single administration of an acetone extract (500 mg/kg) of the herb caused similar effects that were attenuated by pre-treatment with the cytochrome P450 inhibitor piperonyl butoxide (PBO) (*26*). Teucrin A caused mid-zonal hepatic necrosis at 150 mg/kg, comparable to that of the 500 mg/kg dose of the acetone extract (*26*).

For the purpose of our study, male Sprague Dawley rats were orally administered by gavage a single dose of teucrin A (100 mg/kg) and sacrificed after 24 hours. ALT activity in plasma was monitored over 24 hours as a marker of liver toxicity. The dose induced a threefold increase in plasma ALT within 6 hours and by 24 hours the plasma ALT activity was elevated fivefold over control, indicating significant ALT leakage from the injured liver (Figure 7A). The livers were excised and liver homogenates were separated into cytosolic (RLC) and membrane (RLM) fractions by differential centrifugation, such that the membrane fraction contained endoplasmic reticulum, peroxisomal and mitochondrial membranes. RLC and RLM proteins were then separated by SDS-PAGE, transferred to a nitrocellulose membrane and analyzed by Western blotting. To visualize the putative covalent adducts that should form *in vivo* upon metabolism of teucrin A in the liver, we used the periplasmic extracts of the 2I2 ScFv antibody as described above. The 2I2 ScFv was able to selectively detect very low concentrations of teucrin-adducted material in RLC and RLM samples. Immunoreactivity was not observed with untreated RLC and RLM samples. In the treated samples, both cytosolic and membrane proteins were extensively modified by *in vivo* activated teucrin A (Figure 7B).

Immunoprecipitation and LC-MS/MS Analysis of Teucrin A-Adducted Proteins from in Vivo Samples. Using the 2I2 ScFv, immunoprecipitation of the teucrin A-adducted proteins from the rat liver homogenates was performed as described for BSA. In-gel enzymatic digestion of the resulting adduct-enriched protein mixtures was followed by LC-MS/MS analysis. Table 2 lists 46 proteins that were consistently present

in the treated samples from three different animals in duplicate immunoprecipitations and mass spectral analysis. There were 39 unique proteins, which were not detected in the immunoprecipitated samples from the control homogenates. The additional seven proteins (designated with [a] in Table 2) were detected in the control samples, but the enrichment in the treated samples was consistently over fourfold higher, as determined from the increase in the number of unique and total peptides identified per protein, along with an increase in the sequence coverage. Thus, the respective proteins were considered selectively enriched due to modification by the teucrin A metabolite(s). False discovery rates in these experiments were less than 0.5%.

Among the broad range of targets affected most by teucrin A treatment in rat liver were mitochondrial and endoplasmic reticulum (ER) proteins. Damaged mitochondrial proteins included enzymes involved in lipid metabolism, cell respiration and energy production, as well as the essential mitochondrial chaperone Hsp60. Several peroxisomal proteins involved in fatty acid metabolism were identified, as well as catalase, the peroxisomal enzyme responsible for the degradation of hydrogen peroxide. ER-resident proteins adducted by teucrin A represented a number of proteins involved in drug metabolism and clearance, including several cytochrome P450 enzymes, UDP-glucuronosyl transferase and epoxide hydrolase. Additionally, ER proteins with chaperone and maintenance functions were present. Among the cytosolic proteins identified were several proteins involved in amino acid and glucose metabolism, along with glutathione S-transferase M1 and the cytosolic chaperone, Hsp90.

Functional Analysis of the Adducted Proteins Using Ingenuity Pathway Analysis. Two cellular networks were generated through the use of Ingenuity Pathways Analysis (Figure 8A and 8B). The SwissProt gene identifiers of the modified proteins in table *1*, called focus genes, were uploaded into the application and overlaid onto a global molecular network developed from information contained in the Ingenuity Pathways Knowledge Base. The networks were then generated algorithmically based on the connectivity of the focused genes (Table 3). Furthermore, Functional Analysis identified the biological functions and diseases that were most significant to the data set (Table 4).

In Network 1, 14 focused genes were associated with 21 additional genes by direct interactions, which were primarily linked with gene expression, lipid metabolism, and small molecule biochemistry. Figure 8A shows the relations between these focused genes and some important transcriptional regulators involved in the functions associated with Network 1, including peroxisome proliferator-activated receptors (PPAR-α and PPAR-γ), p53 oncogene, transcription factor SP1, sterol regulatory element-binding factor 2 (SREBF2), and tumor suppressor BRCA1. Twelve focused genes were directly linked with 23 genes in the knowledge database, together composing Network 2, primarily associated with lipid metabolism, small molecule biochemistry and drug metabolism. Figure 8B depicts the interactions of these focused genes with transcriptional regulators within this network, such as retinoid X receptor α (RXRA), estrogen receptor (ESR1), hepatocyte nuclear factor 4 α (HNF4α), and transcription factors TCF1, GATA4 and FOS. Network 3 was associated with only five focused genes, which did not achieve statistical significance (< 10). The focused genes involved in Network 3 are mitochondrial proteins Hsp60, carbamoylphosphate synthase, ATP-binding proteins α and β, and cytosolic glyceraldehyde-3-phosphate dehydrogenase. Due to the low score of Network 3, the assignment of focused genes into this network may be coincidental. Table 4 groups the focus genes based on the cellular function or a disease that they are involved in, which is illustrated in figure 8C. The most significant cellular functions are lipid metabolism, small molecule biochemistry, amino acid metabolism, and cellular function and maintenance, followed by drug metabolism and cell death. Among diseases linked to the analyzed focused genes are metabolic, hepatic system and inflammatory disease. Finally, the targets of teucrin A are associated with cellular assembly and organization, molecular transport, cell signaling, and energy production.

Discussion

The identification of protein targets of reactive metabolites of xenobiotics, as well as endogenous reactive products, is becoming the focus of chemical toxicologists in an effort to elucidate the importance of protein adduction in the development of human disease and injury (*52*). Covalent protein adduction correlates with the toxicity of many drugs and xenobiotics, including furan-containing compounds (*53–55*). Furans are activated by cytochrome P450 enzymes into reactive enedial derivatives that are powerful electrophiles, capable of reacting with cellular nucleophiles, including DNA and proteins (*29, 36, 56–62*). Reaction products of several activated furans (such as furan itself and ipomeanol) with model amino acids have been characterized, but the proteins adducted by their toxic metabolites generated *in vivo* and potentially involved in their toxicity remain unidentified (*32, 49*). We previously reported the characterization of the reaction products of **1**, the presumed metabolite of the furano-diterpenoid teucrin A, with NAC and NAL methyl ester, as well as with lysine-containing peptides (*38*). Here, we present identification of the proteins adducted by activated teucrin A *in vivo* in rat liver using a novel approach for the enrichment of teucrin A-adducted proteins that employs an ScFv antibody selected from a rodent phage display library.

Phage display libraries are used for a variety of purposes, ranging from mapping protein-protein interactions, identification of specific binding reagents for receptors and enzymes, determination of enzyme-substrate specificity, and the creation of vaccines (*38, 63–65*). Antibody phage display is perhaps the most common application for the identification of high-affinity specific binding reagents used in the development of human therapeutics and diagnostics, and cell- or tissue-specific markers (*65–68*). The advantage of the phage-displayed antibody library is that the displayed protein is physically linked to the genetic information inside the carrier phage and thus the initial antibody gene inventory can be diversified by recombination, random mutation or site-directed mutagenesis to optimize binding affinity. Consequently, specific antibodies against virtually any target epitope can be isolated very rapidly *in vitro* through phage antibody selection on antigen. This intrinsic quality of phage display technology offers an enormous potential for its use in the identification of protein targets of reactive electrophiles. The ability to synthesize and purify peptide conjugates of activated chemicals provides a means for the generation of structurally characterized epitopes for ScFv antibody selection. Despite the significant potential and versatility of this methodology and its existence for over 20 years, a rather small number of reports describe its application for the detection of specific protein adducts and literature on the use of ScFv antibodies for immunoprecipitation of adducted proteins is unavailable. An ScFv antibody against synthetic peptide conjugates of isoketals, the reactive rearrangement products of F_2-isoprostanes, was

Table 2. Proteins Covalently Modified by Teucrin A in Vivo in the Rat

location	protein	Uniprot/ Swiss-Prot	gene	MW	% sequence coverage (min–max)[b]	no. of unique peptides (min–max)
mitochondria	ATP synthase α-chain, mit.p.	P15999	ATP5A1	59753.6	6.1–12.7	3–7
	ATP synthase β-chain, mit.p.	P10719	ATP5B	56353.6	16.4–21	6–7
	acyl-CoA dehydrogenase, long-chain specific, mit.p.	P15650	ACADL	47872.9	13.3–17.9	4–6
	acyl-CoA dehydrogenase, very long-chain specific, mit.p.	P45953	ACADVL	70749.3	8.5–17.3	5–8
	electron transfer flavoprotein α-subunit, mit.p.	P13803	ETFA	34976.4	21.9–28.8	5–7
	electron transfer flavoprotein, β-polypeptide	Q68FU3	ETFB	27687.4	23.1–27.1	5–5
	hydroxymethylglutaryl-CoA synthase, mit.p.	P22791	HMGCS2	56911.9	13.6–20.7	6–11
	methylmalonate-semialdehyde dehydrogenase, mit.p.	Q02253	ALDH6A1	57807.6	15.5–26.2	7–12
	trifunctional enzyme α subunit, mit.p.	Q64428	HADHA	82512.9	12.6–16.1	7–10
	60 kDa heat shock protein, mit.p. (Hsp60)	P63039	HSPD1	60970.5	5.8–8	3–4
	glutamate dehydrogenase 1, mit.p.	P10860	GLUD1	61427.9	9.7–12.9	4–5
	prohibitin-2 (B-cell receptor-associated protein)	Q5XIH7	PHB2	33312.4	10–13.4	3–4
	3-ketoacyl-CoA thiolase,[a] mit.p.	P13437	ACAA2	41870.9	27.5–39.3	8–10
	aldehyde dehydrogenase,[a] mit.p.	P11884	ALDH2	56488.4	16.4–21.4	8–10
	carbamoyl-phosphate synthase (ammonia),[a] mit.p.	P07756	CPS1	164579.9	25.9–30.1	31–36
ER	78 kDa glucose-regulated protein precursor (GRP78, Bip)	P06761	HSPA5	72347	14.2–23.2	7–11
	NADH-cytochrome b5 reductase (Diaphorase)	P20070	CYB5R3	34255.7	17.5–23.5	4–5
	protein disulfide-isomerase A6 precursor cus	Q63081	PDIA6	48760.2	17.5–25.6	5–7
	retinol dehydrogenase 2	P50170	RDHS	35597.1	24–31.9	7–11
	retinol dehydrogenase 3	P50169	N/A	35662.4	6.3–15.1	2–4
	cytochrome P450 2A1	P11711	CYP2A12	56009.1	7.1–14	3–6
	cytochrome P450 2A2	P15149	CYP2A2	56345.5	6.3–12.6	2–5
	cytochrome P450 2C7	P05179	CYP2C38	56187.1	7.1–12.9	3–4
	cytochrome P450 2D3	P12938	CYP2D13	56641.8	11.6–14.6	5–8
	dimethylaniline monooxygenase (N-oxide-forming) 3	Q9EQ76	FMO3	59960.3	10.2–12.2	5–6
	transitional endoplasmic reticulum ATPase (TER ATPase)	P46462	VCP	89534	4.2–7.5	2–4
	UDP-glucuronosyltransferase 1-1 precursor, microsomal	Q64550	UGT1A1	59662.8	5.4–11.4	3–5
	cytochrome P450 2D1[a]	P10633	CYP2D9	57175.4	24–33.5	12–19
	epoxide hydrolase 1[a]	P07687	EPHX1	52581.6	22.6–27.3	10–13
	fatty aldehyde dehydrogenase[a]	P30839	ALDH3A2	54081.6	14.5–20.9	5–9
peroxisome	acyl-coenzyme A dehydrogenase, short chain	Q6IMX3	N/A	44967.6	6–8.5	2–3
	bile acid CoA:amino acid N-acyltransferase	Q63276	BAAT	46464.7	6.9–14.8	3–5
	catalase	P04762	CAT	59626	6.3–12.7	3–5
	long-chain fatty acid-CoA ligase 1[a]	P18163	ACSL1	78178.7	30.9–33.9	19–20
cytoplasm	4-trimethylaminobutyraldehyde dehydrogenase	Q9JLJ3	ALDH9A1	53652.7	11.3–19.6	4–8
	fructose-bisphosphate aldolase B	P00884	ALDOB	39525	16.8–19	5–6
	argininosuccinate synthase	P09034	ASS	46496.3	13.3–28.2	6–8
	cystathionine γ-lyase	P18757	CTH	43605.3	8.8–15.8	3–5
	glyceraldehyde-3-phosphate dehydrogenase	P04797	GAPDH	35704.9	17.5–24.4	4–5
	heat shock 90 kDa protein 1-β (HSP84)	P34058	HSP90AB1	83341.3	6.8–15.5	4–9
	10-formyltetrahydrofolate dehydrogenase	P28037	ALDH1L1	99126.5	3.7–6.8	2–4
	alcohol dehydrogenase 1	P06757	ADH1C	39514.1	7.2–9.9	3–4
	betaine-homocysteine S-methyltransferase	O09171	BHMT	44976.4	7.1–12.5	3–5
	glutathione S-transferase μ1 (GSTM1-1)	P04905	GSTM5	25894.9	6.4	2
excreted	β2 globin	P11517	HBB	15847.2	34.9–35.6	4–5
	serum paraoxonase/lactonase 3	Q68FP2	PON3	39458.2	10.7	3

[a] Tryptic peptides detected in samples from control animals. Proteins from teucrin A-treated samples were enriched over 4-fold based on peptide count and sequence coverage. [b] Represents the range of minimal to maximal coverage/unique peptide count between three samples obtained from three different animals. Complete MS data are available in the Supporting Information (Table S3a,b).

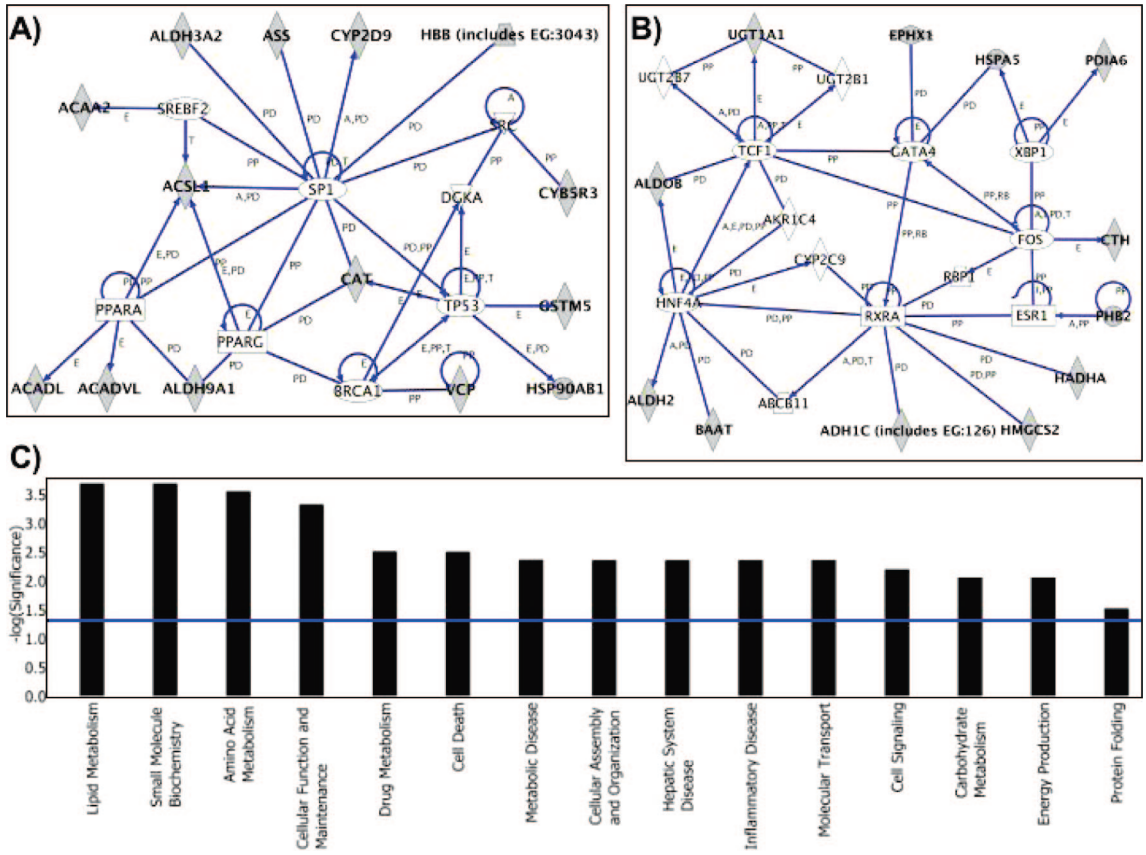

Figure 8. Networks and canonical pathways generated by Ingenuity Pathways Analysis for the targets of teucrin A, called focused genes. (A) The direct interactions between the focused genes (gray) and the transcriptional regulators in network 1. (B) The direct interactions between the focused genes (gray) and the transcriptional regulators in network 2. (C) The cellular pathways, functions, and diseases associated with the focused genes. Abbreviations: A, activation; E, expression; T, transcription; PD, protein–DNA interaction; PP, protein–protein interaction. Network 1: BRCA1, breast cancer 1, early onset; DGKA, diacylglycerol kinase α; PPARA, peroxisome proliferative activated receptor α; PPARG, peroxisome proliferative activated receptor γ; SP1, Sp1 transcription factor; SRC, v-src sarcoma (Schmidt–Ruppin A-2) viral oncogene homologue; SREBF2, sterol regulatory element binding transcription factor 2; TP53, tumor protein 53. Network 2: ABCB11, ATP-binding cassette, subfamily B (MDR/TAP), member 11; AKR1C4, aldo-keto reductase family 1, member C4; CYP2C9, cytochrome P450, family 2, subfamily C, polypeptide 9; ESR1, estrogen receptor 1; FOS, v-fos FBJ murine osteosarcoma viral oncogene homologue; GATA4, GATA binding protein 4; HNF4A, hepatocyte nuclear factor 4α; RXRA, retinoid X receptor α; TCF1, transcription factor 1, hepatic (hepatic nuclear factor HNF1); UGT2B1, UDP glucuronosyltransferase 2 family, polypepetide B1; UGT2B7, UDP glucuronosyltransferase 2 family, polypeptode B7; XBP1, X-box binding protein 1.

Table 3. Genes Directly Associated with the Protein Targets of Teucrin A Metabolite(s) (Bold) Linked to the Affected Cellular Functions by Ingenuity Pathway Analysis

ID	genes	score	focus genes	top functions
1	**ACAA2**, **ACADL**, **ACADVL**, **ACSL1**, **ALDH3A2**, **ALDH9A1**, ANXA8, **ASS**, BRCA1, **CAT**, CTSF (includes EG:8722), **CYB5R3**, **CYP2D9**, CYP4A14, DDIT4, DGKA, FXYD3, **GSTM5**, **HBB** (includes EG:3043), **HSP90AB1**, LHX1, LPIN1, LY6D, MGLL, PERP (includes EG:64065), PEX11A, PHLDA1, PPARA, PPARG, PTPRV, SP1, SRC, SREBF2, TP53, **VCP**	26	14	gene expression, lipid metabolism, small molecule biochemistry
2	ABCB11, **ADH1C** (includes EG:126), AKR1C4, **ALDH2**, **ALDOB**, **BAAT**, **CTH**, CTSL2, **CYP2C9**, **EPHX1**, ESR1, FOS, GATA4, **HADHA**, HMGCS2, HNF4A, **HSPA5**, MPG, NCOA4 (includes EG:8031), NRIP2, PCBD1, **PDIA6**, **PHB2**, PKLR, RBP1, RXRA, SLC10A1, SLC10A2, SNCG, TCF1,**UGT1A1** UGT1A9 (includes EG:54600), UGT2B1, UGT2B7, XBP1	21	12	lipid metabolism, small molecule biochemistry, drug metabolism
3	AR, **ATP5A1**, ATP5A2, **ATP5B**, ATP5C1, ATP5C2, ATP5D, ATP5E, ATP5J, BAX, CA2, CEBPA, **CPS1**, DHFR, FASN, **GAPDH**, GP9, HDAC1 (includes EG:3065), HIST2H2BE, **HSPD1**, MAPKAPK2, MYCN, NFATC1, NFYB, NR3C1, PPARG, PTPN3 (includes EG:5774), RAF1, RIN1, SNCA, TBP, TUBB2A, XRCC5, YWHAG, YWHAZ	7	5	cancer, gene expression, cell cycle

generated and used in tissue samples to visualize the localization of isoketal adducts produced *in vivo* (*39*). In the present study, we synthesized conjugates of enedial derivative of teucrin A with lysine- and cysteine-containing biotinylated peptides, that served as epitopes for the selection of an ScFv antibody that was essentially independent of the peptide sequence and capable of specifically recognizing teucrin A-modified peptides.

To further optimize the ScFv antibody selected in the ELISA for the detection of teucrin A-adducted proteins, we prepared teucrin A enedial **1**-adducted BSA. The adducted BSA was analyzed by LC-MS/MS to determine the modifications. Two equivalents of **1** resulted in the adduction of numerous lysines and one cysteine residue, as listed in Table 1. On the basis of the mass shifts, the conjugates corresponded to the structures **2**

Table 4. Cellular Functions Associated with the Protein Targets of Teucrin A Metabolite(s) Identified by Ingenuity Pathway Analysis

function	significance[a]	genes
amino acid metabolism	2.83×10^{-4}–1.76×10^{-2}	ASS, GLUD1, BAAT, BHMT, CAT
carbohydrate metabolism	8.82×10^{-3}–8.82×10^{-3}	UGT1A1, GAPDH
cell death	3.16×10^{-3}–4.76×10^{-2}	ALDH2, HSPD1, CYB5R3, CAT, HSP90AB1, HADHA, HSPA5, GAPDH
cell signaling	6.36×10^{-3}–8.82×10^{-3}	HSPD1, ASS, CAT
cellular assembly and organization	4.42×10^{-3}–4.33×10^{-2}	ALDOB, VCP, CYB5R3, HSPA5, GAPDH
cellular function and maintenance	4.75×10^{-4}–4.75×10^{-4}	VCP, HSP90AB1, HSPA5
drug metabolism	3.11×10^{-3}–4.76×10^{-2}	CYP2C38, FMO3, CYB5R3, CAT, ADH1C (includes EG:126), RDHS, HSP90AB1, CYP2A12, UGT1A1
endocrine system development and function	3.11×10^{-3}–4.33×10^{-2}	CYB5R3, HSP90AB1, UGT1A1
energy production	8.82×10^{-3}–3.05×10^{-2}	HSPD1, ACADVL, ATP5B
hepatic system disease	4.42×10^{-3}–8.82×10^{-3}	BAAT, CAT, HADHA, UGT1A1
lipid metabolism	2.06×10^{-4}–4.76×10^{-2}	BAAT, ACADVL, HMGCS2, CAT, CYB5R3, ADH1C (includes EG:126), RDHS, HSP90AB1, ACADL, HADHA, ACSL1, UGT1A1
metabolic disease	4.38×10^{-3}–4.42×10^{-3}	ASS, GLUD1, ACADVL, CAT, HADHA, CTH, UGT1A1
molecular transport	4.42×10^{-3}–2.62×10^{-2}	HBB (includes EG:3043), ADH1C (includes EG:126), ACSL1, HADHA, ACADL, UGT1A1, GAPDH
protein folding	3.05×10^{-2}–3.05×10^{-2}	HSP90AB1, PDIA6
small molecule biochemistry	2.06×10^{-4}–4.76×10^{-2}	HSPD1, ALDH2, HBB (includes EG:3043), HMGCS2, BHMT, FMO3, CYB5R3, ADH1C (includes EG:126), HSP90AB1, UGT1A1, ASS, ALDH9A1, GLUD1, BAAT, ACADVL, CAT, RDHS, ACSL1, ACADL, HADHA, ATP5B, GAPDH

[a] Fischer's exact test was used to calculate a p value, determining the probability that the association between the genes in the data set and the canonical pathway is explained by the chance alone.

and **3** in Scheme 2. The residues from the significantly modified peptides are highlighted in the structure of human serum albumin (HSA) in Figure 4 (*50*). It appears that **1** reacts with solvent accessible lysine residues without a considerable selectivity, although a rigorous kinetic analysis was not performed. It is interesting to note that K233 (highlighted in white in Figure 4) is the lysine residue in HSA that is adducted by HNE; this residue does not appear to be a preferential site of modification by **1** (*69*). K233 resides at the end of the fatty acid-binding groove of HSA, which has been proposed to orient the lipid-derived nonpolar HNE molecule and facilitate attack by K233. The diterpenoid structure of teucrin A is polar and is not expected to bind in this hydrophobic region. In addition, **1** appears to be more reactive than HNE (A.D., unpublished observation), and it is likely scavenged by the available nucleophiles before any noncovalent interactions occur. The modified C34, the only free cysteine residue in both HSA and BSA, is a target of many drugs and endogenous cysteine-reactive molecules, as well as oxidative and nitrosative modifications (*70–75*).

The selected ScFv antibody recognized BSA adducted with **1** in the Western blot analysis as shown in Figure 3. The anti-teucrin A ScFv antibody was then used to enrich teucrin A-adducted proteins generated in vivo in rat liver. The list of detected proteins along with their cellular localization is provided in Table 2. Numerous ER-associated proteins were detected in the analysis, among them enzymes involved in xenobiotic metabolism. In particular, the adduction of microsomal epoxide hydrolase (mEH) can be correlated to the interesting observation that autoantibodies against mEH were present in humans who developed hepatitis after exposure to germander preparations (*76, 77*). The formation of autoantibodies supports the idea of covalent adducts playing a role in the development of an immune response against the adducted protein. The sensitivity of mEH may also indicate the involvement of a putative epoxide intermediate as the modifying agent (Scheme 1), although there may be other reasons for the generation of autoantibodies unrelated to modification by germander-derived compounds (*78, 79*). Moreover, among ER-associated proteins detected in our analysis were several cytochrome P450 enzymes (CYP 2A1, 2A2, 2C7, 2D1, and 2D3) and UDP-glucuronosyl transferase 1-1. Interestingly, CYPs as well as UDP-glucuronosyl transferases are targets of autoantibodies in drug-induced hepatitis, further corroborating the possible involvement of the drug-modified proteins in the development of an autoimmune response (*80–82*). Prolonged exposure of the immune system to the peptides generated from degraded modified proteins can lead to the development of immune defense. Besides drug-induced hepatitis, alcohol-induced liver disease also has a strong immune component due to the liver protein damage caused by reactive products of lipid peroxidation arising from the alcohol-initiated oxidative stress (*3, 83, 84*).

Even though teucrin A is activated by CYP 3A in rats, enzymes from this family were not consistently detected in our analysis. This is potentially due to low amounts of these enzymes expressed in rat liver (*85–88*). Unlike in humans, CYP3As are not the major P450 enzymes in rat liver, and to obtain significant expression of these enzymes, induction by phenobarbital or dexamethasone is typically used. However, this was not performed in our experiment. It is also possible that other CYPs are capable of activating teucrin A into electrophilic species, although preliminary in vitro experiments in our laboratory showed complete inhibition of teucrin A metabolism by troleandomycin, a specific CYP3A4 inhibitor, in the presence of other major human CYPs (1A2, 2C8, 2C9, 2C19, 2D6, and 2E1). Interestingly, CYP3A4 was not covalently modified by activated teucrin A in vitro, as determined by Western blot with anti-teucrin A ScFv antibody. Instead, a band with a higher molecular weight showed a signal in the blot (Figure S5, Supporting Information).

Among other ER-associated proteins that were found to be modified by activated teucrin A were proteins with chaperone and maintenance functions, such as GRP78 (BiP), PDI A6, and transitional ER ATPase. GRP78 functions primarily as a chaperone and is an important signaling molecule during reaction to stress (*89–91*). It plays a major role in the initiation of the ER stress response upon accumulation of damaged and unfolded proteins, and it also activates the nutrient deprivation response, in both cases promoting cell survival (*5, 92*). Recently, GRP78 has been identified as a specific proteolytic target of

AB_5 subtilase cytotoxin, a member of the AB_5 family of bacterial toxins such as Schiga, cholera, and pertusis (*93*). The A subunit of AB_5 subtilase is a serine protease that cleaves GRP78 at a single site, resulting in its selective inactivation, thereby triggering death in the target cells. PDIs participate in the correct protein folding of newly synthesized proteins through the maintenance of proper disulfide bridges (*94–97*). GRP78 is among the genes that are significantly up-regulated in response to subtoxic doses of 4-HNE, a lipid peroxidation-derived α,β-unsaturated aldehyde that covalently modifies proteins during oxidative stress (*98*). Additionally, 4-HNE has been shown to covalently modify PDI A6 in vivo and inhibit the enzyme in vitro by modification of a catalytic cysteine residue (*99*). GRP78 and several protein disulfide isomerases, including PDI A6, are also targets of activated BB in vivo (*12, 13*). Transitional ER ATPase (or valosin-containing protein) is involved in the ER, Golgi apparatus, and nuclear envelope membrane fusion, assembly and maintenance, protein transport, and cell cycle regulation (*100–104*). The down-regulation of this protein results in ER membrane swelling. It has numerous chaperone activities, and it is required in ubiquitin-proteasome protein degradation (*105, 106*).

Teucrin A activation resulted in extensive damage of mitochondrial proteins. Several proteins involved in respiration were adducted, including α- and β-chains of ATP synthase, α- and β-subunits of electron-transfer flavoprotein, and trifunctional enzyme, α-subunit. In addition, an essential mitochondrial chaperone, Hsp60, was modified by the teucrin A metabolite(s). A number of enzymes involved in the biosynthesis of fatty acids and small molecule precursors, such as long-chain and very long-chain Acyl-CoA dehydrogenases and carbamoyl-phosphate synthase, respectively, were also adducted. Together, this widespread protein damage may lead to mitochondrial dysfunction. Disruption of mitochondrial function can lead to pore formation and release of cytochrome *c*, resulting in apoptosis. The loss of membrane potential can cause the release of the contents into the cytosol, leading to necrosis. Analogous mechanisms operate in the toxicity of APAP, whose reactive electrophilic metabolite *N*-acetyl-*para*-benzoquinone imine (NAPQI) adducts preferentially mitochondrial proteins involved in respiration (*107*). Among other NAPQI mitochondrial targets found in this study were aldehyde dehydrogenase and glutamate dehydrogenase. Mitochondrial aldehyde dehydrogenase is also covalently modified by 4-HNE and 4-oxononenal (4-ONE), as well as its oxidation product, 4-oxononenoic acid (4-ONEA) (*108*). 4-HNE is a reversible inhibitor of the enzyme that does not modify the active site cysteine residue (Cys302) up to 500 μM concentrations. On the other hand, the more potent irreversible inhibitors 4-ONE and 4-ONEA inhibit the enzyme and covalently bind the active site cysteine at a concentration of 50 μM.

The most abundant protein targets of activated teucrin A in cytosol were enzymes involved in amino acid metabolism, such as argininosuccinate synthase, cystathionine γ-lyase, and betaine-homocysteine *S*-methyltransferase. Two important enzymes involved in the biotransformations of sugars, fructose-biphosphate aldolase B and glyceraldehyde-3-phosphate dehydrogenase, were adducted in our study. Glycolytic enzyme glyceraldehyde-3-phosphate dehydrogenase is also the target of 4-HNE and NAPQI (*109, 110*). 4-HNE inactivates the enzyme in vitro via covalent modification of a surface cysteine and/or histidine residues, whereas NAPQI inactivates it presumably by arylation of Cys-149 in the active site of the enzyme. An important enzyme in purine biosynthesis, 10-formyltetrahydrofolate dehydrogenase (10-FDH), is adducted by teucrin A metabolites, as well as NAPQI (*111*). Covalent modification of 10-FDH can lead to its faster degradation and an up-regulation of new protein synthesis. Ectopic expression of 10-FDH leads to G_1 cell cycle arrest and triggers apoptosis through activation of p53 in cancer cells (*112*).

Among cytosolic chaperones, heat shock protein 90 (Hsp90) was the target of activated teucrin A. Heat shock proteins, such as Hsp90 and Hsp70, bind pro-apoptotic signaling kinases, such as JNK1, and prevent their activation (*5*). Additionally, Hsp90 and Hsp70 bind heat shock factor 1 (HSF1). Covalent damage to these chaperones by electrophiles generated in cells leads to dissociation with their respective binding partners, thus activating their downstream cascades. The release of HSF1 activates the expression of cytoprotective genes, such as chaperones Hsp70 and Hsp40, to boost cellular protection against stress. Hsp90 is also the target of 4-HNE in alcoholic liver disease (*4*). Another cytosolic enzyme essential in the response to electrophilic stress that was adducted by the teucrin A-derived reactive metabolite(s) was glutathione *S*-transferase M1. Aside from its glutathione-conjugating activity, GST M1 regulates certain pro-apoptotic kinases, such ASK1 and MEKK1, via their sequestration into protein complexes (*113, 114*). Modification of critical nucleophilic residues on GST M1 resulting in conformational change is thought to be the mechanism for release of its binding partners, leading to activation of apoptosis (*115*). GSTs are targets for other electrophiles as well. Cysteine 86 of rat GST M1 and to a lesser extent GST M2 is covalently modified in vivo by acrylonitrile, an industrial vinyl monomer that is an acute toxicant and animal carcinogen (*116*). Rat GSTs of class M contain three cysteine residues, C86, C114, and C173, none of which is essential for its catalytic activity as shown by site-directed mutagenesis (*117, 118*). C86 of GST M1 is a preferential site of covalent modification by acrylonitrile because of its lowered pK_a that results from interaction with His 84; this is unique for rat GST M1. NAPQI covalently modifies GST P1 (*119*). The site of modification was not determined. The most reactive cysteine residue in GST P1 is C47, which has an extremely low pK_a due to its interaction with K54 (*120*). Metabolites of BB covalently modify GST A1 and GST A2 at Cys 111 (*121*). 4-HNE covalently binds to and inhibits GSTs in vitro with the order of reactivity and inhibition potency in the presence of GSH being P > A > M, which is changed upon dialysis of GSTs against *S*-hexyl-GSH to A > M > P; this order parallels the number of cysteine residues within the sequence (*122*). The primary GST responsible for GSH conjugation of 4-HNE is GSTA4 (*123, 124*).

Several peroxisomal enzymes also were targets of teucrin A in our study. Among them was catalase, which protects cells from peroxisome-derived hydrogen peroxide (*125, 126*). Covalent modification of this enzyme could lead to its inhibition and an increase in the production of reactive oxygen species, promoting cellular damage. Other peroxisomal targets of activated teucrin A were short-chain acyl-CoA dehydrogenase, bile acid CoA:amino acid *N*-acyltransferase, and long-chain fatty-acid-CoA ligase, all of which are involved in fatty acid biosynthesis. The accumulation of fatty acid due to adduction of fatty acid-metabolizing peroxisomal and mitochondrial proteins can lead to activation of peroxisome proliferator-activating receptor α (PPARα) and peroxisome proliferation, promoting oxidative stress (*127, 128*).

Our results reveal that activation of teucrin A in vivo results in the covalent modification of numerous proteins in the liver. However, despite enrichment of modified proteins using a

specific ScFv antibody, we were not able to demonstrate the presence of teucrin A-modified peptides in the mass spectral experiments. Despite the progress in mass spectrometry methods, identification of modified peptides—the ultimate proof of the modification—remains a challenge, especially in complex in vivo samples. This can be attributed to the dilution effect of the complex peptide mixtures and multiple resultant peptide conjugates, the low level of total covalent binding, and the potential changes in the chromatographic behavior of the modified peptides. Previously reported sites of covalent modification, such as Cys 111 in GST A1 and GST A2 by the benzoquinone metabolite of BB, was possible only after glutathione affinity purification of the GTSs and their chromatographic separation, followed by HPLC linear ion-trap quadrupole Fourier transform mass spectrometry to search for predicted modified tryptic peptides (*121*). Similarly, Cys 86 modified by acrylonitrile in GST M1 was identified after rigorous GST affinity purification and HPLC separation with the help of radiolabeling (*116*).

Together with the results of the current study, it is obvious that diverse reactive intermediates covalently bind similar cellular targets, especially abundant proteins such as chaperones, PDIs, and GSTs. Additionally, the amount of the adduction by agents such as BB or APAP typically does not exceed one modification per 10 protein molecules (*121*). Therefore, the in vivo covalent modification of a protein does not necessarily mean a complete loss of its critical function. However, some reactive metabolites exhibit preferential binding to defined subsets of proteins, which can result in the disruption of the particular cellular function that can have overall detrimental downstream consequences. APAP, in a mouse model of drug-induced liver disease, disrupts mitochondrial function and causes the loss of mitochondrial potential, resulting in the release of cytochrome *c* and the initiation of apoptosis in hepatocytes. This correlates well with the ability of NAPQI to preferentially bind to mitochondrial proteins involved in respiration. The structural analogue of APAP, 3′-hydroxyacetanilid (AMAP), is also metabolized by P450s into the electrophilic species, 2-acetamido-*para*-benzoquinone. While the covalent binding of NAPQI to proteins correlates with the liver toxicity observed after APAP overdose, AMAP is not toxic despite the covalent binding of its metabolite to proteins (*129*). The metabolite of AMAP preferentially modifies cytosolic proteins in hepatocytes. Although the functional significance of these observations is uncertain, the differences in the toxicity profiles of the two compounds and the subcellular targets of the two quinones are evident.

The importance of characterizing the complete spectrum of modified proteins by different reactive intermediates is critical to determining the mechanisms of toxicity induced by protein damage. Additionally, it will be important to assess the enzymatic activity of the protein targets to determine the relevance of the covalent binding in toxicity. A more complete understanding of these processes could be achieved with the knowledge of the proteome changes following the exposure to the reactive intermediates. We are currently investigating the effects of the toxic dose of teucrin A on individual protein levels in rat liver. Knowledge databases, such as Ingenuity Pathway Analysis used in this study, will be an essential tool for finding the linkages between the protein targets and the proteome and gene expression changes induced by reactive intermediates and for understanding the cellular pathways responsible for their action.

Our current results illustrate that antibody phage display technology is a potentially powerful approach for studying protein adduction by miscellaneous compounds. Antibody selection is accomplished by rapid panning methodologies that employ rigorously identified peptide adduct antigens. No in vivo immunizations are required, and the stability and thereby identity of the antigen are unequivocally established. Multiple strategies are available to optimize the affinity of the selected antibody for the antigen. Using an anti-teucrin A-specific ScFv, we showed that teucrin A covalently modifies proteins following activation in the rat liver in vivo. Immunoenrichment of the adducted proteins with the ScFv antibody enabled us to identify a broad range of protein targets of the teucrin A metabolite(s) in vivo in rat liver. We were able to show that mitochondrial and ER-associated proteins are the major targets of teucrin A, along with enzymes involved in cell maintenance and small molecule metabolism. This study represents the first complete proteomic analysis of the in vivo protein targets of an activated furan-containing xenobiotic.

Acknowledgment. This work was supported by research grants from the National Foundation for Cancer Research and the National Institute of Health (ES-013125).

Supporting Information Available: Detailed mass spectrometric analysis of the peptide fragments of target proteins. This information is available free of charge via the Internet at http://pubs.acs.org.

References

(1) Guengerich, F. P., and Liebler, D. C. (1985) Enzymatic activation of chemicals to toxic metabolites. *Crit. Rev. Toxicol. 14*, 259–307.
(2) Pumford, N. R. (1997) Protein targets of xenobiotic reactive intermediates. *Annu. Rev. Pharmacol. Toxicol. 37*, 91–117.
(3) Petersen, D. R., and Doorn, J. A. (2004) Reactions of 4-hydroxynonenal with proteins and cellular targets. *Free Radical Biol. Med. 37*, 937–945.
(4) Carbone, D. L., Doorn, J. A., Kiebler, Z., Ickes, B. R., and Petersen, D. R. (2005) Modification of heat shock protein 90 by 4-hydroxynonenal in a rat model of chronic alcoholic liver disease. *J. Pharmacol. Exp. Ther. 315*, 8–15.
(5) West, J. D., and Marnett, L. J. (2006) Endogenous reactive intermediates as modulators of cell signaling and cell death. *Chem. Res. Toxicol. 19*, 173–194.
(6) Evans, D. C., Watt, A. P., Nicoll-Griffith, D. A., and Baillie, T. A. (2004) Drug-protein adducts: An industry perspective on minimizing the potential for drug bioactivation in drug discovery and development. *Chem. Res. Toxicol. 17*, 3–16.
(7) Baillie, T. A., Cayen, M. N., Fouda, H., Gerson, R. J., Green, J. D., Grossman, S. J., Klunk, L. J., LeBlanc, B., Perkins, D. G., and Shipley, L. A. (2002) Drug metabolites in safety testing. *Toxicol. Appl. Pharmacol. 182*, 188–196.
(8) Baillie, T. A., and Kassahun, K. (2001) Biological reactive intermediates in drug discovery and development: A perspective from the pharmaceutical industry. *Adv. Exp. Med. Biol. 500*, 45–51.
(9) Carbone, D. L., Doorn, J. A., and Petersen, D. R. (2004) 4-Hydroxynonenal regulates 26S proteasomal degradation of alcohol dehydrogenase. *Free Radical Biol. Med. 37*, 1430–1439.
(10) Thome-Kromer, B., Bonk, I., Klatt, M., Nebrich, G., Taufmann, M., Bryant, S., Wacker, U., and Kopke, A. (2003) Toward the identification of liver toxicity markers: A proteome study in human cell culture and rats. *Proteomics 3*, 1835–62.
(11) Sampey, B. P., Korourian, S., Ronis, M. J., Badger, T. M., and Petersen, D. R. (2003) Immunohistochemical characterization of hepatic malondialdehyde and 4-hydroxynonenal modified proteins during early stages of ethanol-induced liver injury. *Alcohol Clin. Exp. Res. 27*, 1015–1022.
(12) Koen, Y. M., and Hanzlik, R. P. (2002) Identification of seven proteins in the endoplasmic reticulum as targets for reactive metabolites of bromobenzene. *Chem. Res. Toxicol. 15*, 699–706.
(13) Koen, Y. M., Williams, T. D., and Hanzlik, R. P. (2000) Identification of three protein targets for reactive metabolites of bromobenzene in rat liver cytosol. *Chem. Res. Toxicol. 13*, 1326–1335.
(14) Rombach, E. M., and Hanzlik, R. P. (1999) Detection of adducts of bromobenzene 3,4-oxide with rat liver microsomal protein sulfhydryl groups using specific antibodies. *Chem. Res. Toxicol. 12*, 159–163.

(15) Hartley, D. P., Kolaja, K. L., Reichard, J., and Petersen, D. R. (1999) 4-Hydroxynonenal and malondialdehyde hepatic protein adducts in rats treated with carbon tetrachloride: Immunochemical detection and lobular localization. *Toxicol. Appl. Pharmacol. 161*, 23–33.
(16) Rombach, E. M., and Hanzlik, R. P. (1998) Identification of a rat liver microsomal esterase as a target protein for bromobenzene metabolites. *Chem. Res. Toxicol. 11*, 178–184.
(17) Hartley, D. P., and Petersen, D. R. (1997) Profiles of hepatic cellular protein adduction by malondialdehyde and 4-hydroxynonenal. Studies with isolated hepatocytes. *Adv. Exp. Med. Biol. 414*, 123–131.
(18) Hartley, D. P., Kroll, D. J., and Petersen, D. R. (1997) Prooxidant-initiated lipid peroxidation in isolated rat hepatocytes: Detection of 4-hydroxynonenal- and malondialdehyde-protein adducts. *Chem. Res. Toxicol. 10*, 895–905.
(19) Hartley, D. P., Lindahl, R., and Petersen, D. R. (1995) Covalent modification of class 2 and class 3 aldehyde dehydrogenase by 4-hydroxynonenal. *Adv. Exp. Med. Biol. 372*, 93–101.
(20) Bambal, R. B., and Hanzlik, R. P. (1995) Bromobenzene 3,4-oxide alkylates histidine and lysine side chains of rat liver proteins in vivo. *Chem. Res. Toxicol. 8*, 729–735.
(21) Slaughter, D. E., and Hanzlik, R. P. (1991) Identification of epoxide- and quinone-derived bromobenzene adducts to protein sulfur nucleophiles. *Chem. Res. Toxicol. 4*, 349–359.
(22) Narasimhan, N., Weller, P. E., Buben, J. A., Wiley, R. A., and Hanzlik, R. P. (1988) Microsomal metabolism and covalent binding of [3H/14C]-bromobenzene. Evidence for quinones as reactive metabolites. *Xenobiotica 18*, 491–499.
(23) De Vincenzi, M., Maialetti, F., and Silano, M. (2003) Constituents of aromatic plants: Teucrin A. *Fitoterapia 74*, 746–749.
(24) Bedir, E., Manyam, R., and Khan, I. A. (2003) Neo-clerodane diterpenoids and phenylethanoid glycosides from *Teucrium chamaedrys* L. *Phytochemistry 63*, 977–983.
(25) Kouzi, S. A., McMurtry, R. J., and Nelson, S. D. (1994) Hepatotoxicity of germander (*Teucrium chamaedrys* L.) and one of its constituent neoclerodane diterpenes teucrin A in the mouse. *Chem. Res. Toxicol. 7*, 850–856.
(26) Lekehal, M., Pessayre, D., Lereau, J. M., Moulis, C., Fouraste, I., and Fau, D. (1996) Hepatotoxicity of the herbal medicine germander: Metabolic activation of its furano diterpenoids by cytochrome P450 3A Depletes cytoskeleton-associated protein thiols and forms plasma membrane blebs in rat hepatocytes. *Hepatology 24*, 212–218.
(27) Fau, D., Lekehal, M., Farrell, G., Moreau, A., Moulis, C., Feldmann, G., Haouzi, D., and Pessayre, D. (1997) Diterpenoids from germander, an herbal medicine, induce apoptosis in isolated rat hepatocytes. *Gastroenterology 113*, 1334–1346.
(28) Boyd, M. R., Grygiel, J. J., and Minchin, R. F. (1983) Metabolic activation as a basis for organ-selective toxicity. *Clin. Exp. Pharmacol. Physiol. 10*, 87–99.
(29) Falzon, M., McMahon, J. B., Schuller, H. M., and Boyd, M. R. (1986) Metabolic activation and cytotoxicity of 4-ipomeanol in human non-small cell lung cancer lines. *Cancer Res. 46*, 3484–3489.
(30) Baertschi, S. W., Raney, K. D., Stone, M. P., and Harris, T. M. (1988) Preparation of the 8,9-epoxide of the mycotoxin aflatoxin b_1: The ultimate carcinogenic species. *J. Am. Chem. Soc. 110*, 7929–7931.
(31) Smela, M. E., Currier, S. S., Bailey, E. A., and Essigmann, J. M. (2001) The chemistry and biology of aflatoxin B (1): From mutational spectrometry to carcinogenesis. *Carcinogenesis 22*, 535–545.
(32) Baer, B. R., Rettie, A. E., and Henne, K. R. (2005) Bioactivation of 4-ipomeanol by CYP4B1: Adduct characterization and evidence for an enedial intermediate. *Chem. Res. Toxicol. 18*, 855–864.
(33) Dalvie, D. K., Kalgutkar, A. S., Khojasteh-Bakht, S. C., Obach, R. S., and O'Donnell, J. P. (2002) Biotransformation reactions of five-membered aromatic heterocyclic rings. *Chem. Res. Toxicol. 15*, 269–299.
(34) Thomassen, D., Knebel, N., Slattery, J. T., McClanahan, R. H., and Nelson, S. D. (1992) Reactive intermediates in the oxidation of menthofuran by cytochromes P-450. *Chem. Res. Toxicol. 5*, 123–130.
(35) McClanahan, R. H., Thomassen, D., Slattery, J. T., and Nelson, S. D. (1989) Metabolic activation of (*R*)-(+)-pulegone to a reactive enonal that covalently binds to mouse liver proteins. *Chem. Res. Toxicol. 2*, 349–355.
(36) Ravindranath, V., Burka, L. T., and Boyd, M. R. (1984) Reactive metabolites from the bioactivation of toxic methylfurans. *Science 224*, 884–886.
(37) Chen, L. J., Hecht, S. S., and Peterson, L. A. (1995) Identification of cis-2-butene-1,4-dial as a microsomal metabolite of furan. *Chem. Res. Toxicol. 8*, 903–906.
(38) Druckova, A., and Marnett, L. J. (2006) Characterization of the amino acid adducts of the enedial derivative of teucrin A. *Chem. Res. Toxicol. 19*, 1330–1340.
(39) Davies, S. S., Talati, M., Wang, X., Mernaugh, R. L., Amarnath, V., Fessel, J., Meyrick, B. O., Sheller, J., and Roberts, L. J. (2004) Localization of isoketal adducts in vivo using a single-chain antibody. *Free Radical Biol. Med. 36*, 1163–1174.
(40) Murray, R. W., and Jeyaraman, R. (1985) Dioxiranes—Synthesis and reactions of methyldioxiranes. *J. Org. Chem. 50*, 2847–2853.
(41) Pope, T., Embelton, J., and Mernaugh, R. L. (1996) Construction and use of antibody gene repertories. In *Antibody Engineering: A Practical Approach* (McCafferty, J., Chiswell, D., and Hoogenboom, H., Eds.) IRL Press, Oxford, England.
(42) Vinion-Dubiel, A. D., McClain, M. S., Cao, P., Mernaugh, R. L., and Cover, T. L. (2001) Antigenic diversity among *Helicobacter pylori* vacuolating toxins. *Infect. Immun. 69*, 4329–4336.
(43) Lapierre, L. A., Avant, K. M., Caldwell, C. M., Ham, A. J., Hill, S., Williams, J. A., Smolka, A. J., and Goldenring, J. R. (2007) Characterization of immunoisolated human gastric parietal cells tubulovesicles: Identification of regulators of apical recycling. *Am. J. Physiol. Gastrointest. Liver Physiol. 292* (5), G1249–62.
(44) Ham, A.-J. (2005) Proteolytic digestion protocols. In *The Encyclopedia of Mass Spectrometry, Volume 2 Biological Applications Part A: Proteins and Peptides* (Caprioli, R. M., and Gross, M. L., Eds.) Vol. 2, pp 10–17, Elsevier Ltd., Kidlington, Oxford, United Kingdom.
(45) Cortes, H. J., Pfeiffer, C. D., Richter, B. E., and Stevens, T. S. (1987) Porous ceramic bed supports for fused-silica packed capillary columns used in liquid-chromatography. *J. High Resolut. Chromatogr. Chromatogr. Commun. 10*, 446–448.
(46) Licklider, L.J., Thoreen, C. C., Peng, J. M., and Gygi, S. P. (2002) Automation of nanoscale microcapillary liquid chromatography-tandem mass spectromentry with a vented column. *Anal. Chem. 74*, 3076–3083.
(47) Yates, J. R., Eng, J. K., Mccormack, A. L., and Schieltz, D. (1995) Method to correlate tandem mass-spectra of modified peptides to amino-acid-sequences in the protein database. *Anal. Chem. 67*, 1426–1436.
(48) Elias, J. E., Haas, W., Faherty, B. K., and Gygi, S. P. (2005) Comparative evaluation of mass spectrometry platforms used in large-scale proteomics investigations. *Nat. Methods 2*, 667–675.
(49) Chen, L. J., Hecht, S. S., and Peterson, L. A. (1997) Characterization of amino acid and glutathione adducts of *cis*-2-butene-1,4-dial, a reactive metabolite of furan. *Chem. Res. Toxicol. 10*, 866–874.
(50) He, X. M., and Carter, D. C. (1992) Atomic structure and chemistry of human serum albumin. *Nature 358*, 209–215.
(51) Loeper, J., Descatoire, V., Letteron, P., Moulis, C., Degott, C., Dansette, P., Fau, D., and Pessayre, D. (1994) Hepatotoxicity of germander in mice. *Gastroenterology 106*, 464–472.
(52) Baillie, T. A. (2006) Future of toxicology—Metabolic activation and drug design: Challenges and apportunities in chemical toxicology. *Chem. Res. Toxicol. 19*, 889–893.
(53) Pumford, N. R., Halmes, N. C., and Hinson, J. A. (1997) Covalent binding of xenobiotics to specific proteins in the liver. *Drug Metab. Rev. 29*, 39–57.
(54) Guengerich, F. P. (2005) Principles of covalent binding of reactive metabolites and examples of activation of bis-electrophiles by conjugation. *Arch. Biochem. Biophys. 433*, 369–378.
(55) Boyd, M. R. (1981) Toxicity mediated by reactive metabolites of furans. *Adv. Exp. Med. Biol. 136* (Part B), 865–879.
(56) Gordon, W. P., Huitric, A. C., Seth, C. L., McClanahan, R. H., and Nelson, S. D. (1987) The metabolism of the abortifacient terpene, (*R*)-(+)-pulegone, to a proximate toxin, menthofuran. *Drug Metab. Dispos. 15*, 589–594.
(57) Kobayashi, T., Sugihara, J., and Harigaya, S. (1987) Mechanism of metabolic cleavage of a furan ring. *Drug Metab. Dispos. 15*, 877–881.
(58) Parmar, D., and Burka, L. T. (1993) Studies on the interaction of furan with hepatic cytochrome P-450. *J. Biochem. Toxicol. 8*, 1–9.
(59) Sahali-Sahly, Y., Balani, S. K., Lin, J. H., and Baillie, T. A. (1996) In vitro studies on the metabolic activation of the furanopyridine L-754,394, a highly potent and selective mechanism-based inhibitor of cytochrome P450 3A4. *Chem. Res. Toxicol. 9*, 1007–1012.
(60) Racha, J. K., Rettie, A. E., and Kunze, K. L. (1998) Mechanism-based inactivation of human cytochrome P450 1A2 by furafylline: Detection of a 1:1 adduct to protein and evidence for the formation of a novel imidazomethide intermediate. *Biochemistry 37*, 7407–7419.
(61) Zhang, K. E., Naue, J. A., Arison, B., and Vyas, K. P. (1996) Microsomal metabolism of the 5-lipoxygenase inhibitor L-739,010: Evidence for furan bioactivation. *Chem. Res. Toxicol. 9*, 547–554.
(62) Boyd, M. R., and Dutcher, J. S. (1981) Renal toxicity due to reactive metabolites formed in situ in the kidney: Investigations with 4-ipomeanol in the mouse. *J. Pharmacol. Exp. Ther. 216*, 640–646.
(63) Smothers, J. F., Henikoff, S., and Carter, P. (2002) Tech.Sight. Phage display. Affinity selection from biological libraries. *Science 298*, 621–622.
(64) Smothers, J. F., and Henikoff, S. (2001) Predicting in vivo protein peptide interactions with random phage display. *Comb. Chem. High Throughput Screening 4*, 585–591.

(65) Yip, Y. L., and Ward, R. L. (1999) Epitope discovery using monoclonal antibodies and phage peptide libraries. *Comb. Chem. High Throughput Screening 2*, 125–138.
(66) Wang, L. F., and Yu, M. (2004) Epitope identification and discovery using phage display libraries: Applications in vaccine development and diagnostics. *Curr. Drug Targets 5*, 1–15.
(67) Mancini, N., Carletti, S., Perotti, M., Canducci, F., Mammarella, M., Sampaolo, M., and Burioni, R. (2004) Phage display for the production of human monoclonal antibodies against human pathogens. *New Microbiol. 27*, 315–328.
(68) Azzazy, H. M., and Highsmith, W. E., Jr (2002) Phage display technology: Cclinical applications and recent innovations. *Clin. Biochem. 35*, 425–445.
(69) Szapacs, M. E., Riggins, J. N., Zimmerman, L. J., and Liebler, D. C. (2006) Covalent adduction of human serum albumin by 4-hydroxy-2-nonenal: kinetic analysis of competing alkylation reactions. *Biochemistry 45*, 10521–10528.
(70) Ivanov, A. I., Christodoulou, J., Parkinson, J. A., Barnham, K. J., Tucker, A., Woodrow, J., and Sadler, P. J. (1998) Cisplatin binding sites on human albumin. *J. Biol. Chem. 273*, 14721–14730.
(71) Fabisiak, J. P., Sedlov, A., and Kagan, V. E. (2002) Quantification of oxidative/nitrosative modification of CYS(34) in human serum albumin using a fluorescence-based SDS-PAGE assay. *Antioxid. Redox Signaling 4*, 855–865.
(72) Shen, B., and English, A. M. (2005) Mass spectrometric analysis of nitroxyl-mediated protein modification: Comparison of products formed with free and protein-based cysteines. *Biochemistry 44*, 14030–14044.
(73) Talib, J., Beck, J. L., and Ralph, S. F. (2006) A mass spectrometric investigation of the binding of gold antiarthritic agents and the metabolite [Au(CN)2]- to human serum albumin. *J. Biol. Inorg. Chem. 11*, 559–570.
(74) Ascoli, G. A., Domenici, E., and Bertucci, C. (2006) Drug binding to human serum albumin: Abridged review of results obtained with high-performance liquid chromatography and circular dichroism. *Chirality 18*, 667–679.
(75) Bertucci, C., and Domenici, E. (2002) Reversible and covalent binding of drugs to human serum albumin: Methodological approaches and physiological relevance. *Curr. Med. Chem. 9*, 1463–1481.
(76) De Berardinis, V., Moulis, C., Maurice, M., Beaune, P., Pessayre, D., Pompon, D., and Loeper, J. (2000) Human microsomal epoxide hydrolase is mthe target of germander-induced autoantibodies on the surface of human hepatocytes. *Mol. Pharmacol. 58*, 542–551.
(77) Loeper, J., De Berardinis, V., Moulis, C., Beaune, P., Pessayre, D., and Pompon, D. (2001) Human epoxide hydrolase is the target of germander autoantibodies on the surface of human hepatocytes: Enzymatic implications. *Adv. Exp. Med. Biol. 500*, 121–124.
(78) Boitier, E., and Beaune, P. (2000) Xenobiotic-metabolizing enzymes as autoantigens in human autoimmune disorders. An update. *Clin. Rev. Allergy Immunol. 18*, 215–239.
(79) Strassburg, C. P., Obermayer-Straub, P., and Manns, M. P. (2000) Autoimmunity in liver diseases. *Clin. Rev. Allergy Immunol. 18*, 127–139.
(80) Boitier, E., and Beaune, P. (1999) Cytochromes P450 as targets to autoantibodies in immune mediated diseases. *Mol. Aspects Med. 20*, 84–137.
(81) Mizutani, T., Shinoda, M., Tanaka, Y., Kuno, T., Hattori, A., Usui, T., Kuno, N., and Osaka, T. (2005) Autoantibodies against CYP2D6 and other drug-metabolizing enzymes in autoimmune hepatitis type 2. *Drug Metab. Rev. 37*, 235–252.
(82) Obermayer-Straub, P., Strassburg, C. P., and Manns, M. P. (2000) Target proteins in human autoimmunity: cytochromes P450 and UDP-glucuronosyltransferases. *Can. J. Gastroenterol. 14*, 429–439.
(83) Mottaran, E., Stewart, S. F., Rolla, R., Vay, D., Cipriani, V., Moretti, M., Vidali, M., Sartori, M., Rigamonti, C., Day, C. P., and Albano, E. (2002) Lipid peroxidation contributes to immune reactions associated with alcoholic liver disease. *Free Radical Biol. Med. 32*, 38–45.
(84) Stewart, S. F., Vidali, M., Day, C. P., Albano, E., and Jones, D. E. (2004) Oxidative stress as a trigger for cellular immune responses in patients with alcoholic liver disease. *Hepatology 39*, 197–203.
(85) Corcos, L., and Lagadic-Gossmann, D. (2001) Gene induction by phenobarbital: An update on an old question that receives key novel answers. *Pharmacol. Toxicol. 89*, 113–122.
(86) Czekaj, P. (2000) Phenobarbital-induced expression of cytochrome P450 genes. *Acta Biochim. Pol. 47*, 1093–1105.
(87) Gibson, G. G., Plant, N. J., Swales, K. E., Ayrton, A., and El-Sankary, W. (2002) Receptor-dependent transcriptional activation of cytochrome P4503A genes: Induction mechanisms, species differences and interindividual variation in man. *Xenobiotica 32*, 165–206.
(88) Joannard, F., Galisteo, M., Corcos, L., Guillouzo, A., and Lagadic-Gossmann, D. (2000) Regulation of phenobarbital-induction of CYP2B and CYP3A genes in rat cultured hepatocytes: Involvement of several serine/threonine protein kinases and phosphatases. *Cell. Biol. Toxicol. 16*, 325–337.
(89) Haas, I. G. (1994) BiP (GRP78), an essential hsp70 resident protein in the endoplasmic reticulum. *Experientia 50*, 1012–1020.
(90) Kleizen, B., and Braakman, I. (2004) Protein folding and quality control in the endoplasmic reticulum. *Curr. Opin. Cell Biol. 16*, 343–349.
(91) Sommer, T., and Jarosch, E. (2002) BiP binding keeps ATF6 at bay. *Dev. Cell 3*, 1–2.
(92) Zhang, K., and Kaufman, R. J. (2006) Protein folding in the endoplasmic reticulum and the unfolded protein response. *Handb. Exp. Pharmacol.* 69–91.
(93) Paton, A. W., Beddoe, T., Thorpe, C. M., Whisstock, J. C., Wilce, M. C., Rossjohn, J., Talbot, U. M., and Paton, J. C. (2006) AB5 subtilase cytotoxin inactivates the endoplasmic reticulum chaperone BiP. *Nature 443*, 548–552.
(94) Cribb, A. E., Peyrou, M., Muruganandan, S., and Schneider, L. (2005) The endoplasmic reticulum in xenobiotic toxicity. *Drug Metab. Rev. 37*, 405–442.
(95) Ellgaard, L., and Ruddock, L. W. (2005) The human protein disulphide isomerase family: Substrate interactions and functional properties. *EMBO Rep. 6*, 28–32.
(96) Sitia, R., and Molteni, S. N. (2004) Stress, protein (mis)folding, and signaling: The redox connection. *Sci. STKE* pe27.
(97) Wilkinson, B., and Gilbert, H. F. (2004) Protein disulfide isomerase. *Biochim. Biophys. Acta 1699*, 35–44.
(98) West, J. D., and Marnett, L. J. (2005) Alterations in gene expression induced by the lipid peroxidation product, 4-hydroxy-2-nonenal. *Chem. Res. Toxicol. 18*, 1642–1653.
(99) Carbone, D. L., Doorn, J. A., Kiebler, Z., and Petersen, D. R. (2005) Cysteine modification by lipid peroxidation products inhibits protein disulfide isomerase. *Chem. Res. Toxicol. 18*, 1324–1331.
(100) Bruderer, R. M., Brasseur, C., and Meyer, H. H. (2004) The AAA ATPase p97/VCP interacts with its alternative co-factors, Ufd1-Npl4 and p47, through a common bipartite binding mechanism. *J. Biol. Chem. 279*, 49609–49616.
(101) Cao, K., Nakajima, R., Meyer, H. H., and Zheng, Y. (2003) The AAA-ATPase Cdc48/p97 regulates spindle disassembly at the end of mitosis. *Cell 115*, 355–367.
(102) Hetzer, M., Meyer, H. H., Walther, T. C., Bilbao-Cortes, D., Warren, G., and Mattaj, I. W. (2001) Distinct AAA-ATPase p97 complexes function in discrete steps of nuclear assembly. *Nat. Cell Biol. 3*, 1086–1091.
(103) Patel, S., and Latterich, M. (1998) The AAA team: related ATPases with diverse functions. *Trends Cell Biol. 8*, 65–71.
(104) Ye, Y., Meyer, H. H., and Rapoport, T. A. (2001) The AAA ATPase Cdc48/p97 and its partners transport proteins from the ER into the cytosol. *Nature 414*, 652–656.
(105) Wang, Q., Song, C., and Li, C. C. (2004) Molecular perspectives on p97-VCP: Progress in understanding its structure and diverse biological functions. *J. Struct. Biol. 146*, 44–57.
(106) Dai, R. M., and Li, C. C. (2001) Valosin-containing protein is a multi-ubiquitin chain-targeting factor required in ubiquitin-proteasome degradation. *Nat. Cell Biol. 3*, 740–744.
(107) Qiu, Y., Benet, L. Z., and Burlingame, A. L. (1998) Identification of the hepatic protein targets of reactive metabolites of acetaminophen in vivo in mice using two-dimensional gel electrophoresis and mass spectrometry. *J. Biol. Chem. 273*, 17940–17953.
(108) Doorn, J. A., Hurley, T. D., and Petersen, D. R. (2006) Inhibition of human mitochondrial aldehyde dehydrogenase by 4-hydroxynon-2-enal and 4-oxonon-2-enal. *Chem. Res. Toxicol. 19*, 102–110.
(109) Dietze, E. C., Schafer, A., Omichinski, J. G., and Nelson, S. D. (1997) Inactivation of glyceraldehyde-3-phosphate dehydrogenase by a reactive metabolite of acetaminophen and mass spectral characterization of an arylated active site peptide. *Chem. Res. Toxicol. 10*, 1097–1103.
(110) Uchida, K., and Stadtman, E. R. (1993) Covalent attachment of 4-hydroxynonenal to glyceraldehyde-3-phosphate dehydrogenase. A possible involvement of intra- and intermolecular cross-linking reaction. *J. Biol. Chem. 268*, 6388–6393.
(111) Pumford, N. R., Halmes, N. C., Martin, B. M., Cook, R. J., Wagner, C., and Hinson, J. A. (1997) Covalent binding of acetaminophen to N-10-formyltetrahydrofolate dehydrogenase in mice. *J. Pharmacol. Exp. Ther. 280*, 501–505.
(112) Oleinik, N. V., and Krupenko, S. A. (2003) Ectopic expression of 10-formyltetrahydrofolate dehydrogenase in A549 cells induces G1 cell cycle arrest and apoptosis. *Mol. Cancer Res. 1*, 577–588.
(113) Cho, S. G., Lee, Y. H., Park, H. S., Ryoo, K., Kang, K. W., Park, J., Eom, S. J., Kim, M. J., Chang, T. S., Choi, S. Y., Shim, J., Kim, Y., Dong, M. S., Lee, M. J., Kim, S. G., Ichijo, H., and Choi, E. J. (2001) Glutathione S-transferase mu modulates the stress-activated signals by suppressing apoptosis signal-regulating kinase 1. *J. Biol. Chem. 276*, 12749–12755.

(114) Ryoo, K., Huh, S. H., Lee, Y. H., Yoon, K. W., Cho, S. G., and Choi, E. J. (2004) Negative regulation of MEKK1-induced signaling by glutathione S-transferase Mu. *J. Biol. Chem. 279*, 43589–43594.

(115) Dorion, S., Lambert, H., and Landry, J. (2002) Activation of the p38 signaling pathway by heat shock involves the dissociation of glutathione S-transferase Mu from Ask1. *J. Biol. Chem. 277*, 30792–30797.

(116) Nerland, D. E., Cai, J., Pierce, W. M., Jr., and and Benz, F. W. (2001) Covalent binding of acrylonitrile to specific rat liver glutathione S-transferases in vivo. *Chem. Res. Toxicol. 14*, 799–806.

(117) Hsieh, J. C., Huang, S. C., Chen, W. L., Lai, Y. C., and Tam, M. F. (1991) Cysteine-86 is not needed for the enzymic activity of glutathione S-transferase 3-3. *Biochem. J. 278* (Part 1), 293–297.

(118) Chen, W. L., Hsieh, J. C., Hong, J. L., Tsai, S. P., and Tam, M. F. (1992) Site-directed mutagenesis and chemical modification of cysteine residues of rat glutathione S-transferase 3-3. *Biochem. J. 286* (Part 1), 205–210.

(119) Ozdemirler, G., Aykac, G., Uysal, M., and Oz, H. (1994) Liver lipid peroxidation and glutathione-related defence enzyme systems in mice treated with paracetamol. *J. Appl. Toxicol. 14*, 297–299.

(120) Vega, M. C., Walsh, S. B., Mantle, T. J., and Coll, M. (1998) The three-dimensional structure of Cys-47-modified mouse liver glutathione S-transferase P1-1. Carboxymethylation dramatically decreases the affinity for glutathione and is associated with a loss of electron density in the alphaB-310B region. *J. Biol. Chem. 273*, 2844–2850.

(121) Koen, Y. M., Yue, W., Galeva, N. A., Williams, T. D., and Hanzlik, R. P. (2006) Site-specific arylation of rat glutathione s-transferase A1 and A2 by bromobenzene metabolites in vivo. *Chem. Res. Toxicol. 19*, 1426–1434.

(122) Mitchell, A. E., Morin, D., Lame, M. W., and Jones, A. D. (1995) Purification, mass spectrometric characterization, and covalent modification of murine glutathione S-transferases. *Chem. Res. Toxicol. 8*, 1054–1062.

(123) Berhane, K., Widersten, M., Engstrom, A., Kozarich, J. W., and Mannervik, B. (1994) Detoxication of base propenals and other alpha, beta-unsaturated aldehyde products of radical reactions and lipid peroxidation by human glutathione transferases. *Proc. Natl. Acad. Sci. U.S.A. 91*, 1480–1484.

(124) Hartley, D. P., Ruth, J. A., and Petersen, D. R. (1995) The hepatocellular metabolism of 4-hydroxynonenal by alcohol dehydrogenase, aldehyde dehydrogenase, and glutathione S-transferase. *Arch. Biochem. Biophys. 316*, 197–205.

(125) Chelikani, P., Fita, I., and Loewen, P. C. (2004) Diversity of structures and properties among catalases. *Cell Mol. Life Sci. 61*, 192–208.

(126) Kahl, R., Kampkotter, A., Watjen, W., and Chovolou, Y. (2004) Antioxidant enzymes and apoptosis. *Drug Metab. Rev. 36*, 747–762.

(127) Gonzalez, F. J., Peters, J. M., and Cattley, R. C. (1998) Mechanism of action of the nongenotoxic peroxisome proliferators: role of the peroxisome proliferator-activator receptor alpha. *J. Natl. Cancer Inst. 90*, 1702–1709.

(128) Reddy, J. K. (2004) Peroxisome proliferators and peroxisome proliferator-activated receptor alpha: Biotic and xenobiotic sensing. *Am. J. Pathol. 164*, 2305–2321.

(129) Qiu, Y., Benet, L. Z., and Burlingame, A. L. (2001) Identification of hepatic protein targets of the reactive metabolites of the non-hepatotoxic regioisomer of acetaminophen, 3′-hydroxyacetanilide, in the mouse in vivo using two-dimensional gel electrophoresis and mass spectrometry. *Adv. Exp. Med. Biol. 500*, 663–673.

TX7001405